SANDIA REPORT
SAND2021-5331
Printed April 2021

Sandia National Laboratories

SAR Geolocation Using Range-Only Multilateration

Armin W Doerry and Douglas L Bickel

Prepared by
Sandia National Laboratories
Albuquerque, New Mexico
87185 and Livermore,
California 94550

Issued by Sandia National Laboratories, operated for the United States Department of Energy by National Technology & Engineering Solutions of Sandia, LLC.

Available to DOE and DOE contractors from
U.S. Department of Energy
Office of Scientific and Technical Information
P.O. Box 62
Oak Ridge, TN 37831

Telephone: (865) 576-8401
Facsimile: (865) 576-5728
E-Mail: reports@osti.gov
Online ordering: http://www.osti.gov/scitech

Available to the public from
U.S. Department of Commerce
National Technical Information Service
5301 Shawnee Rd
Alexandria, VA 22312

Telephone: (800) 553-6847
Facsimile: (703) 605-6900
E-Mail: orders@ntis.gov
Online order: https://classic.ntis.gov/help/order-methods/

SAR Geolocation Using Range-Only Multilateration

Armin W Doerry and Douglas L Bickel

Abstract

Radar is by its basic nature a ranging instrument. If radar range measurements from multiple directions can be made and assembled, then multilateration allows locating a feature common to the set of Synthetic Aperture Radar (SAR) images to an accurate 3-D coordinate. The ability to employ effective multilateration algorithms is highly dependent on the geometry of the data collections, and the accuracy with which relative range measurements can be made. The problem can be cast as a least-squares exercise, and the concept of Dilution of Precision can describe the accuracy and precision with which a 3-D location can be made.

Acknowledgements

This report is the result of an unfunded Research and Development effort.

The authors thank their colleague Tim Bielek for his review of this report and appreciated comments.

Contents

Acronyms and Definitions 7
Foreword 8
Classification 8
Author Contact Information 8
1 Introduction and Background 9
2 Basic Trilateration 11
2.1 Extension to Arbitrary Multilateration 15
2.2 Weighted Least Squares Solution 16
2.3 Dilution of Precision (DOP) 18
2.4 Multilateration Examples 21
2.4.1 Straight-line Collection Geometry 21
2.4.2 Circular Orbit Arc 22
3 Multilateration with a Range Bias 25
3.1 Dilution of Precision (DOP) 29
3.2 Multilateration Examples 30
3.2.1 Circular Orbit Arc 30
3.2.2 Spiral Arc 32
4 Multilateration with a Tethered Range Bias 35
4.1 Weighted Least Squares Solution 37
4.2 Dilution of Precision (DOP) 38
4.3 Multilateration Examples 39
4.3.1 Circular Orbit Arc 39
4.3.2 Spiral Arc 41
5 Differential Geolocation 43
6 Differential Ranging 47
7 Factors Influencing Accurate Radar Ranging 51
Combined Ranging Errors 53
8 Conclusions 55
Appendix A – Basic Linear Algebra 57
Appendix B – Dilution of Precision (DOP) 59
Appendix C – Range Bias Due to Atmosphere 63
Variation in Surface Refractivity 64
Variation in Range Bias 65
Comments 65
Reference 67
Distribution 70

List of Figures

Figure 1. Geometry of geolocation problem. 11
Figure 2. Straight-line data collection geometry. All numerical values in meters. 21
Figure 3. Circular Orbit Arc collection geometry. All numerical values in meters. 22
Figure 4. Circular Orbit Arc collection geometry. All numerical values in meters. 30
Figure 5. Spiral Arc collection geometry. All numerical values in meters. 32
Figure 6. Circular Orbit Arc collection geometry. All numerical values in meters. 39
Figure 7. Spiral Arc collection geometry. All numerical values in meters. 41
Figure 8. RMS range error as a function of range. Radar is assumed at 3000 m altitude. 53
Figure 9. Campsite in the mountains (courtesy Miss Taylor Spaulding, 7 ½). 56
Figure 10. Relationship of range bias factor with altitude for various surface refractivities. 66
Figure 11. Estimated standard deviation of range bias factor as a function of altitude. 66

List of Tables

Table 1. Sample results from a set of independent experimental simulations where noise with a standard deviation of 0.1 m was added to the range measurements. Scatterer true location is at $\mathbf{s} = \begin{bmatrix} 3 & 2 & 1 \end{bmatrix}^T$ 23

Table 2. Sample results from a set of independent experimental simulations where noise with a standard deviation of 0.1 m was added to the range measurements. Scatterer true location is at $\mathbf{s} = \begin{bmatrix} 3 & 2 & 1 \end{bmatrix}^T$ with a constant range bias of 3 m. 33

Table 3. Sample results from a set of independent experimental simulations where noise with a standard deviation of 0.1 m was added to the range measurements, and range bias truth varied with a standard deviation of 0.4 m. Scatterer true location is at $\mathbf{s} = \begin{bmatrix} 3 & 2 & 1 \end{bmatrix}^T$ with tethered range bias of 3 m. 40

Table 4. Sample results from a set of independent experimental simulations where noise with a standard deviation of 0.1 m was added to the range measurements, and range bias truth varied with a standard deviation of 0.4 m. Scatterer true location is at $\mathbf{s} = \begin{bmatrix} 3 & 2 & 1 \end{bmatrix}^T$ with a constant range bias of 3 m. 42

Acronyms and Definitions

1-D, 2-D, 3-D	1-, 2-, 3-Dimesional
APC	Antenna Phase Center
DOA	Direction of Arrival
DOP	Dilution of Precision
GDOP	Geometric DOP
GPS	Global Positioning System
HDOP	Horizontal DOP
INS	Inertial Navigation System
MIG	Multiple-Image Geopositioning
MMSE	Minimum Mean Squared Error
NGA	National Geospatial-Intelligence Agency
PDOP	Position DOP
RMS	Root Mean Square
RSS	Root Sum Squared
SAR	Synthetic Aperture Radar
SIG	Single-Image Geopositioning
SRP	Scene Reference Point
TDOP	Time DOP
VDOP	Vertical DOP

Foreword

This report details the results of an academic study. It does not presently exemplify any modes, methodologies, or techniques employed by any operational system known to the authors.

Classification

The specific mathematics and algorithms presented herein do not bear any release restrictions or distribution limitations.

This report formalizes preexisting informal notes and other documentation on the subject matter herein.

This report has been approved as Unclassified – Unlimited Release.

Author Contact Information

Armin Doerry	awdoerr@sandia.gov	505-845-8165
Doug Bickel	dlbicke@sandia.gov	505-845-9038

1 Introduction and Background

Synthetic Aperture Radar (SAR) is a coherent imaging technique whereby maps of radar reflectivity are made from radar echo soundings along some flight path. Note that a SAR image is essentially a 2-D projection of a 3-D scene. The utility of the SAR image is considerably enhanced with accurate and precise geolocation of the image, especially features in the image.

Radar is by its basic nature a ranging instrument. In fact, the final "r" in the acronym "radar" is for "ranging." If radar range measurements from multiple directions can be made and assembled, then the prospect of using multilateration might allow locating a feature common to a set of SAR images to an accurate 3-D coordinate for that feature.

To be sure, the ability to employ effective multilateration algorithms is highly dependent on the geometry of the data collections, and the accuracy with which relative range measurements can be made.

We offer as relevant background information the following publications.

> SAND99-2643 details a stereoscopic technique for height estimation from two SAR images.[1]
>
> SAND2001-2585 extends the stereoscopic technique to more than two images.[2]
>
> SAND2013-1096 details effects of the atmosphere on radar ranging.[3]
>
> SAND2012-10690 details refraction more generally in the atmosphere.[4]
>
> SAND2020-10779 discusses the impact of radar motion measurement errors on single-image geolocation accuracy.[5]
>
> SAND2021-0144 discusses the effects of geometry on Height of Focus for SAR images.[6]
>
> In his Ph.D. dissertation, Wonnacott discusses in detail geolocation from spotlight SAR images.[7]

Herein this report we will assume that multiple range measurements will be made from independent SAR images over a set of viewing directions, and that those range measurements are independent and noncoherent in characteristic. As such this constitutes a Multiple-Image Geopositioning (MIG) problem versus a Single-Image Geopositioning (SIG) problem.

We will ignore any Direction of Arrival (DOA) measurements due to Doppler or other interferometry within an image, generally relying on range measurements only. We will also assume that the feature of interest in the set of SAR images is accurately identified, and corresponded in the image set. Techniques for selecting a common feature with accuracy and precision, and establishing correspondence across the images, are beyond the scope of this report.

This report will further assess the “goodness” of various data collection geometries, using a Dilution of Precision (DOP) measure.

Finally, we note that radar-based geolocation is of particular interest to the US National Geospatial-Intelligence Agency (NGA), who publishes standards in the area, including SAR-based Geopositioning.[8]

2 Basic Trilateration

Our intent is to discern the spatial location of some radar scatterer, or retroreflector. The true geolocation of the scatterer is specified by a vector containing three coordinate coefficients. Finding these three unknowns requires three suitable independent measurements. The geometry of our problem is given in Figure 1.

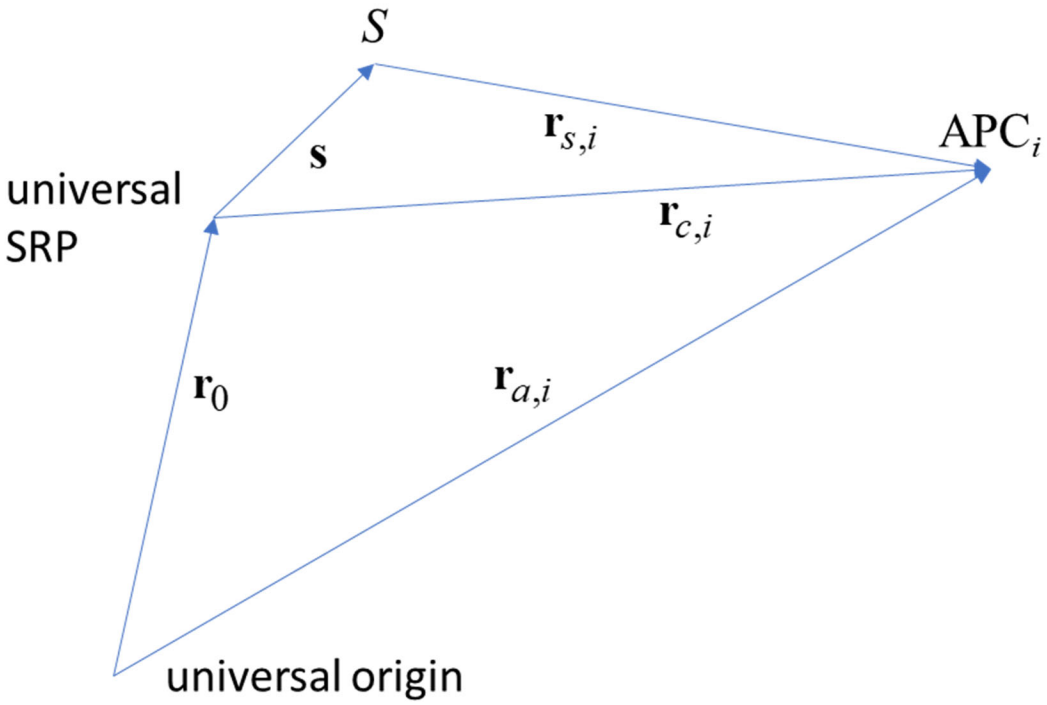

Figure 1. Geometry of geolocation problem.

We accordingly define some specific locations as

> Universal Origin = the origin of a common coordinate system (e.g. earth center),
> Universal SRP = some common Scene Reference Point (SRP),
> S = scattering location to be geolocated, and
> APC$_i$ = Antenna Phase Center (APC) at i^{th} radar position for a ranging measurement. (1)

The Universal Origin for our purposes is somewhat arbitrary. It is defined for us mainly as a reference for any position/motion measurements of the radar.

The Universal SRP is a reference location, expected to be within the neighborhood of the scattering location to be geolocated. It might be the SRP for one or more of the SAR images, or not. For our problem it is defined at the beginning of the data analysis.

These positions allow us to define specific vectors as

$\mathbf{r}_0$ = vector from Universal Origin to Universal SRP,
$\mathbf{s}$ = vector from Universal SRP to the scattering location *S*, and
$\mathbf{r}_{a,i}$ = vector from Universal Origin to the i^{th} radar position measurement. (2)

The vector $\mathbf{r}_{a,i}$ is measured by the radar's motion measurement, or navigation subsystem.

These vectors allow us to calculate

$\mathbf{r}_{c,i} = \mathbf{r}_{a,i} - \mathbf{r}_0$ = vector from Universal SRP to i^{th} radar position APC$_i$,
$\mathbf{r}_{s,i} = \mathbf{r}_{c,i} - \mathbf{s}$ = vector from scattering location *S* to i^{th} radar position APC$_i$. (3)

The radar, by means of its echolocation, attempts to measure the magnitude of $\mathbf{r}_{s,i}$, namely

$\left|\mathbf{r}_{s,i}\right|$ = what the radar attempts to measure with its echo range soundings. (4)

We may expand our radar measurements to

$$\left|\mathbf{r}_{s,i}\right|^2 = \left|\mathbf{r}_{c,i} - \mathbf{s}\right|^2 = \left(\mathbf{r}_{c,i} - \mathbf{s}\right) \bullet \left(\mathbf{r}_{c,i} - \mathbf{s}\right) = \left|\mathbf{r}_{c,i}\right|^2 + \left|\mathbf{s}\right|^2 - 2\mathbf{r}_{c,i} \bullet \mathbf{s} \,. \tag{5}$$

This may be rearranged and rewritten as

$$\mathbf{r}_{c,i} \bullet \mathbf{s} = \mathbf{r}_{c,i}{}^T \mathbf{s} = \frac{1}{2}\left(\left|\mathbf{r}_{c,i}\right|^2 - \left|\mathbf{r}_{s,i}\right|^2 + \left|\mathbf{s}\right|^2\right), \tag{6}$$

where the "T" superscript denotes transpose.

Given three radar positions with independent measurements, we may construct the matrix equation

$$\begin{bmatrix} \mathbf{r}_{c,1}{}^T \\ \mathbf{r}_{c,2}{}^T \\ \mathbf{r}_{c,3}{}^T \end{bmatrix} \mathbf{s} = \begin{bmatrix} \frac{1}{2}\left(\left|\mathbf{r}_{c,1}\right|^2 - \left|\mathbf{r}_{s,1}\right|^2 + \left|\mathbf{s}\right|^2\right) \\ \frac{1}{2}\left(\left|\mathbf{r}_{c,2}\right|^2 - \left|\mathbf{r}_{s,2}\right|^2 + \left|\mathbf{s}\right|^2\right) \\ \frac{1}{2}\left(\left|\mathbf{r}_{c,3}\right|^2 - \left|\mathbf{r}_{s,3}\right|^2 + \left|\mathbf{s}\right|^2\right) \end{bmatrix}. \tag{7}$$

This equation is of the well-known form

$$\mathbf{A}\,\mathbf{s} = \mathbf{b}\,, \tag{8}$$

where the matrices and vectors are identified as

$$\mathbf{A} = \begin{bmatrix} \mathbf{r}_{c,1}{}^T \\ \mathbf{r}_{c,2}{}^T \\ \mathbf{r}_{c,3}{}^T \end{bmatrix} = 3\times3 \text{ square matrix, and}$$

$$\mathbf{b} = \begin{bmatrix} \frac{1}{2}\left(|\mathbf{r}_{c,1}|^2 - |\mathbf{r}_{s,1}|^2 + |\mathbf{s}|^2 \right) \\ \frac{1}{2}\left(|\mathbf{r}_{c,2}|^2 - |\mathbf{r}_{s,2}|^2 + |\mathbf{s}|^2 \right) \\ \frac{1}{2}\left(|\mathbf{r}_{c,3}|^2 - |\mathbf{r}_{s,3}|^2 + |\mathbf{s}|^2 \right) \end{bmatrix} = 3\times1 \text{ column vector.} \tag{9}$$

If **A** has full rank, it has an inverse, and we may calculate the 3-D geolocation of scattering location *S* as

$$\mathbf{s} = \mathbf{A}^{-1}\mathbf{b}, \tag{10}$$

just like back in engineering school, except that we have a few minor issues to take care of first.

Some Comments on Calculating a Solution

We offer the following comments.

- First, we note that our **b** vector contains $|\mathbf{s}|^2$, which is of course a function of the thing we are trying to calculate. We might treat this in any of several ways,
    a. We might simply ignore it, and accept the error it generates in our calculations.
    b. We might use an approximation of **s**, based on its location on one or more of the SAR images.
    c. We might iterate our calculation to continuously improve our estimate of **s**. Our calculation algorithm would then become
        1. Within the **b** vector set $\mathbf{s} = \begin{bmatrix} 0 & 0 & 0 \end{bmatrix}^T$.
        2. Calculate a new **s** vector using Eq. (10).
        3. Use the new **s** vector to construct a new **b** vector using Eq. (9).
        4. Go back to step 2, iterating until convergence.

        Anecdotally, convergence is typically very quick to sub-millimeter accuracy.
    d. We might use an elimination method, as shown later in Section 6, or in a paper by Manolakis.[9]

- Second, we are presuming that the radar can reasonably accurately measure range $\left|\mathbf{r}_{s,i}\right|$.

  This isn't always as easy as it might seem. A radar "measures" range by measuring an echo time delay and assuming a propagation velocity for the radar waveform round trip. In fact, even the measured time delay is really a measure of clock cycles of an assumed stable clock period. Many radar systems assume a free-space velocity of propagation, and ignore the slowing of this velocity due to atmospheric dielectric properties, which may slow propagation by several hundred parts per million. This of course causes a range error, perhaps significant, unless compensated in some manner.[3] Although an exact value for the resulting range error is unknowable to the radar, we can often improve our estimate to some degree by making intelligent assumptions for atmospheric properties, and compensating accordingly. In addition, imprecise knowledge of transmission delays within the radar hardware itself will also cause uncertainties in a radar's range "measurement." Such hardware delays can be mitigated with good radar calibration.[10]

- Third, we are presuming that our navigation subsystem can reasonably accurately measure radar position $\mathbf{r}_{a,i}$, and by extension $\mathbf{r}_{c,i}$. A good GPS-aided Inertial Navigation System (INS) will typically be able to keep any navigation errors fairly small, often in the meter range with a high degree of temporal correlation.[5] For analysis, radar position errors are often combined with radar range measurement errors.

- Fourth, to make Eq. (10) work at all, matrix **A** must have full rank. Even better, we would like **A** to be well-conditioned to better tolerate input measurement errors. Since **A** is essentially a function of radar positions, i.e. flight path, this means that the "goodness" of our geolocation is highly dependent on the data collection geometry, i.e. the geometry of the radar positions.

  For example, if all APC_i are colinear, matrix **A** is singular, and hence not invertible. This means a collection geometry that involves radar locations on a straight line is not adequate for geolocation. Even a "nearly" straight-line radar collection geometry will result in an ill-conditioned matrix **A**, still too unsuitable for adequate geolocation.

  Furthermore, in fact, even if not colinear, if all APC_i are merely coplanar with the Universal SRP, then **A** is again effectively singular, and hence not invertible. This means essentially if we need to calculate a 3-D solution for **s**, then **A** needs to be invertible, which in turn means that we need radar positions that are not coplanar; we need out-of-plane ranging measurements.[†]

[†] Out-of-plane means that if two radar positions with the Universal SRP define a plane, then the third radar position needs to be not in this plane.

2.1 Extension to Arbitrary Multilateration

The preceding development assumed exactly three measurements for calculating the three unknown coordinates of **s**. We now allow for more than three measurements to calculate **s**, in a Minimum Mean Squared Error (MMSE) sense. Let us now assume M independent range measurements from M radar positions. The over-constrained matrix equation becomes

$$\begin{bmatrix} \mathbf{r}_{c,1}{}^T \\ \mathbf{r}_{c,2}{}^T \\ \vdots \\ \mathbf{r}_{c,M}{}^T \end{bmatrix} \mathbf{s} = \begin{bmatrix} \frac{1}{2}\left(|\mathbf{r}_{c,1}|^2 - |\mathbf{r}_{s,1}|^2 + |\mathbf{s}|^2 \right) \\ \frac{1}{2}\left(|\mathbf{r}_{c,2}|^2 - |\mathbf{r}_{s,2}|^2 + |\mathbf{s}|^2 \right) \\ \vdots \\ \frac{1}{2}\left(|\mathbf{r}_{c,M}|^2 - |\mathbf{r}_{s,M}|^2 + |\mathbf{s}|^2 \right) \end{bmatrix}. \tag{11}$$

This equation is still of the form

$$\mathbf{A}\,\mathbf{s} = \mathbf{b}\,, \tag{12}$$

where

$$\mathbf{A} = \begin{bmatrix} \mathbf{r}_{c,1}{}^T \\ \mathbf{r}_{c,2}{}^T \\ \vdots \\ \mathbf{r}_{c,M}{}^T \end{bmatrix} = M \times 3 \text{ matrix, and}$$

$$\mathbf{b} = \begin{bmatrix} \frac{1}{2}\left(|\mathbf{r}_{c,1}|^2 - |\mathbf{r}_{s,1}|^2 + |\mathbf{s}|^2 \right) \\ \frac{1}{2}\left(|\mathbf{r}_{c,2}|^2 - |\mathbf{r}_{s,2}|^2 + |\mathbf{s}|^2 \right) \\ \vdots \\ \frac{1}{2}\left(|\mathbf{r}_{c,M}|^2 - |\mathbf{r}_{s,M}|^2 + |\mathbf{s}|^2 \right) \end{bmatrix} = M \times 1 \text{ column vector.} \tag{13}$$

If **A** has full column rank (independent columns), it has a pseudo-inverse, and we may calculate the MMSE geolocation of scattering location S as

$$\hat{\mathbf{s}} = \left(\mathbf{A}^T \mathbf{A} \right)^{-1} \mathbf{A}^T \mathbf{b}\,. \tag{14}$$

We note that our **b** vector still contains $|\mathbf{s}|^2$, which can be treated in the same manner as for $M = 3$ above. In fact, the solution for $M = 3$ is just a special case of Eq. (14), meaning that Eq. (14) is valid for $M \geq 3$, noting that for the case $M = 3$ and full-rank **A**, we equate

$$\left(\mathbf{A}^T \mathbf{A} \right)^{-1} \mathbf{A}^T = \mathbf{A}^{-1}, \qquad \text{for full-rank square } \mathbf{A}. \tag{15}$$

2.2 Weighted Least Squares Solution

The solution in Eq. (14) tacitly assumes that all observations of $\left|\mathbf{r}_{s,i}\right|$ are equally accurate and precise in a statistical sense. This may be a reasonable assumption if all the $\left|\mathbf{r}_{s,i}\right|$ are of a similar magnitude. However, if there is a substantial spread in $\left|\mathbf{r}_{s,i}\right|$ magnitudes, then this assumption may not be quite right. Indeed, ranges will vary, and the nature of many sources of error in range calculations are somewhat range dependent, often increasing the error with range.

Consider that an error in $\left|\mathbf{r}_{s,i}\right|$ will cause an error in the **b** vector as

$$\mathbf{b}+\boldsymbol{\varepsilon}_b = \begin{bmatrix} \frac{1}{2}\left(\left|\mathbf{r}_{c,1}\right|^2 - \left(\left|\mathbf{r}_{s,1}\right| + \varepsilon_{s,1}\right)^2 + \left|\mathbf{s}\right|^2\right) \\ \frac{1}{2}\left(\left|\mathbf{r}_{c,2}\right|^2 - \left(\left|\mathbf{r}_{s,2}\right| + \varepsilon_{s,2}\right)^2 + \left|\mathbf{s}\right|^2\right) \\ \vdots \\ \frac{1}{2}\left(\left|\mathbf{r}_{c,M}\right|^2 - \left(\left|\mathbf{r}_{s,M}\right| + \varepsilon_{s,M}\right)^2 + \left|\mathbf{s}\right|^2\right) \end{bmatrix}, \tag{16}$$

where

$$\begin{aligned} \boldsymbol{\varepsilon}_b &= \text{the resulting error in } \mathbf{b}, \text{ and} \\ \varepsilon_{s,i} &= \text{the error in the measure of } \left|\mathbf{r}_{s,i}\right|. \end{aligned} \tag{17}$$

From this, we may relate

$$\boldsymbol{\varepsilon}_b = \begin{bmatrix} -\left(\left|\mathbf{r}_{s,1}\right|\varepsilon_{s,1} + \frac{1}{2}{\varepsilon_{s,1}}^2\right) \\ -\left(\left|\mathbf{r}_{s,2}\right|\varepsilon_{s,2} + \frac{1}{2}{\varepsilon_{s,2}}^2\right) \\ \vdots \\ -\left(\left|\mathbf{r}_{s,M}\right|\varepsilon_{s,M} + \frac{1}{2}{\varepsilon_{s,M}}^2\right) \end{bmatrix} \approx \begin{bmatrix} -\left|\mathbf{r}_{s,1}\right|\varepsilon_{s,1} \\ -\left|\mathbf{r}_{s,2}\right|\varepsilon_{s,2} \\ \vdots \\ -\left|\mathbf{r}_{s,M}\right|\varepsilon_{s,M} \end{bmatrix}, \tag{18}$$

noting that the squared-error terms are expected to be tiny by comparison. We will presume that the errors are independent, hence uncorrelated. While a credible argument can be made that some degree of correlation in these errors might be expected, we will forego this complication and leave a calculation of its effects as an exercise for the reader. For our immediate purposes, assuming uncorrelated errors is adequate.

The covariance of $\boldsymbol{\varepsilon}_b$ may then be calculated as

$$\boldsymbol{\Sigma}_b = E\left\{\boldsymbol{\varepsilon}_b \boldsymbol{\varepsilon}_b{}^T\right\} \approx E\left\{\text{diag}\left(\left[\left(\left|\mathbf{r}_{s,1}\right|^2 \varepsilon_{s,1}{}^2\right) \quad \left(\left|\mathbf{r}_{s,2}\right|^2 \varepsilon_{s,2}{}^2\right) \quad \cdots \quad \left(\left|\mathbf{r}_{s,M}\right|^2 \varepsilon_{s,M}{}^2\right)\right]\right)\right\}. \quad (19)$$

This may be written as

$$\boldsymbol{\Sigma}_b = \text{diag}\left(\left[\left(\left|\mathbf{r}_{s,1}\right|^2 \sigma_{s,1}^2\right) \quad \left(\left|\mathbf{r}_{s,2}\right|^2 \sigma_{s,2}^2\right) \quad \cdots \quad \left(\left|\mathbf{r}_{s,M}\right|^2 \sigma_{s,M}^2\right)\right]\right), \quad (20)$$

where

$$\sigma_{s,i}^2 = E\left\{\varepsilon_{s,i}^2\right\} = \text{the variance in the individual range measurements.} \quad (21)$$

This allows us to write the covariance matrix $\boldsymbol{\Sigma}_b$ as

$$\boldsymbol{\Sigma}_b = \left|\mathbf{r}_{s,ref}\right|^2 \sigma_{ref}^2 \mathbf{K}, \quad (22)$$

where

$$\mathbf{K} = \text{diag}\left(\left[\left(\frac{\left|\mathbf{r}_{s,1}\right|^2 \sigma_{s,1}^2}{\left|\mathbf{r}_{s,ref}\right|^2 \sigma_{ref}^2}\right) \quad \left(\frac{\left|\mathbf{r}_{s,2}\right|^2 \sigma_{s,2}^2}{\left|\mathbf{r}_{s,ref}\right|^2 \sigma_{ref}^2}\right) \quad \cdots \quad \left(\frac{\left|\mathbf{r}_{s,M}\right|^2 \sigma_{s,M}^2}{\left|\mathbf{r}_{s,ref}\right|^2 \sigma_{ref}^2}\right)\right]\right),$$

σ_{ref}^2 = nominal reference variance for measured range error, and

$\left|\mathbf{r}_{s,ref}\right|$ = nominal reference range. (23)

The variation in variance at different ranges is manifest in matrix **K**. Consequently, we may choose a weighting matrix for a weighted least-squares solution to be

$$\mathbf{W} = \mathbf{K}^{-1} = \text{diag}\left(\left[\left(\frac{\left|\mathbf{r}_{s,1}\right|^2 \sigma_{s,1}^2}{\left|\mathbf{r}_{s,ref}\right|^2 \sigma_{ref}^2}\right)^{-1} \quad \left(\frac{\left|\mathbf{r}_{s,2}\right|^2 \sigma_{s,2}^2}{\left|\mathbf{r}_{s,ref}\right|^2 \sigma_{ref}^2}\right)^{-1} \quad \cdots \quad \left(\frac{\left|\mathbf{r}_{s,M}\right|^2 \sigma_{s,M}^2}{\left|\mathbf{r}_{s,ref}\right|^2 \sigma_{ref}^2}\right)^{-1}\right]\right). \quad (24)$$

Using this we may calculate the weighted least-squares solution to be

$$\hat{\mathbf{s}} = \left(\mathbf{A}^T \mathbf{W} \mathbf{A}\right)^{-1} \mathbf{A}^T \mathbf{W} \mathbf{b}, \quad (25)$$

where optimal weights are given in Eq. (24).

We note that this weighting is related to "whitening" techniques in signal processing.

2.3 Dilution of Precision (DOP)

Dilution of Precision (DOP) is a figure of merit for a linear system that relates an output standard deviation to an input standard deviation. Accordingly, using the results in Appendix B, we identify the output covariance matrix as

$$\mathbf{\Sigma}_s = \mathbf{C}\,\mathbf{\Sigma}_b\,\mathbf{C}^T, \tag{26}$$

where generally for a weighted least-squares solution

$$\mathbf{C} = \left(\mathbf{A}^T\mathbf{W}\mathbf{A}\right)^{-1}\mathbf{A}^T\mathbf{W}, \tag{27}$$

and $\mathbf{\Sigma}_b$ is the same as in the previous section, above. Expanding Eq. (26) using Eq. (22) yields

$$\mathbf{\Sigma}_s = \sigma_{ref}^2\left|\mathbf{r}_{s,ref}\right|^2\mathbf{C}\,\mathbf{K}\,\mathbf{C}^T. \tag{28}$$

Normalizing to σ_{ref}^2 yields

$$\frac{\mathbf{\Sigma}_s}{\sigma_{ref}^2} = \left|\mathbf{r}_{s,ref}\right|^2\mathbf{C}\,\mathbf{K}\,\mathbf{C}^T. \tag{29}$$

The square-root of the diagonal elements of $\mathbf{\Sigma}_s/\sigma_{ref}^2$ are the DOP values, with the constraint that they are generally relative to $\left|\mathbf{r}_{s,ref}\right|$ and σ_{ref}^2, depending on how we define the **K** matrix. We will write this as

$$\mathbf{d}_{DOP} = \mathrm{diag}\left(\frac{\mathbf{\Sigma}_s}{\sigma_{ref}^2}\right)^{1/2}, \tag{30}$$

understanding that the square-root operation is on elements of the diagonal. The DOP values themselves are then a ratio of standard deviations.

Comments

At ranges of a few tens of km, in a well-calibrated radar, with ranges compensated for atmospheric propagation (discussed in more detail later in Section 7) the bulk of the variances $\sigma_{s,i}^2$ are probably due to the accuracy and precision of the position of the radar, APC$_i$.

Consequently, it is not unreasonable to assume that all $\sigma_{s,i}^2$ are somewhat equal, and may reasonably be represented with a common representative variance, so that

$$\sigma_{s,i}^2 = \sigma_{s,j}^2 = \sigma_{ref}^2. \tag{31}$$

Case 1. Simple Constant Range Collection

We note that for a simple uniformly weighted case where $\mathbf{K} = \mathbf{W} = \mathbf{I}$, then Eq. (29) reduces to

$$\frac{\boldsymbol{\Sigma}_s}{\sigma_{ref}^2} = \left|\mathbf{r}_{s,ref}\right|^2 \left(\mathbf{A}^T\mathbf{A}\right)^{-1}. \tag{32}$$

This, of course, assumes that for all range measurements $\mathbf{r}_{s,i}$, the products of squared ranges and variances are equal, that is

$$\left|\mathbf{r}_{s,i}\right|^2 \sigma_{s,i}^2 = \left|\mathbf{r}_{s,ref}\right|^2 \sigma_{ref}^2 . \tag{33}$$

A sufficient condition for Eq. (33) to hold is that ranges themselves are equal, and the variance in their measurements are equal, namely

$$\begin{aligned} &\sigma_{s,i}^2 = \sigma_{ref}^2 \text{ = constant, and} \\ &\left|\mathbf{r}_{s,i}\right| = \left|\mathbf{r}_{s,ref}\right| \text{ = constant.} \end{aligned} \tag{34}$$

Case 2. Simple Variable Range Collection

We now examine the case where variances are equal for each measurement, but the ranges may vary, namely where

$$\begin{aligned} &\sigma_{s,i}^2 = \sigma_{ref}^2 \text{ = constant and} \\ &\left|\mathbf{r}_{s,i}\right| \text{ = independent and not necessarily constant.} \end{aligned} \tag{35}$$

In this case the specific choice for $\left|\mathbf{r}_{s,ref}\right|$ can be somewhat arbitrary, as whatever value we choose will cancel in the final calculation anyway. This allows us to calculate

$$\mathbf{K} = \text{diag}\left(\left[\left(\frac{\left|\mathbf{r}_{s,1}\right|^2}{\left|\mathbf{r}_{s,ref}\right|^2}\right) \left(\frac{\left|\mathbf{r}_{s,2}\right|^2}{\left|\mathbf{r}_{s,ref}\right|^2}\right) \cdots \left(\frac{\left|\mathbf{r}_{s,M}\right|^2}{\left|\mathbf{r}_{s,ref}\right|^2}\right)\right]\right). \tag{36}$$

If we assume uniform weighting, such that $\mathbf{W} = \mathbf{I}$, then Eq. (29) becomes

$$\frac{\boldsymbol{\Sigma}_s}{\sigma_{ref}^2} = \left|\mathbf{r}_{s,ref}\right|^2 \left(\mathbf{A}^T\mathbf{A}\right)^{-1} \mathbf{A}^T \ \mathbf{K}\mathbf{A} \left(\mathbf{A}^T\mathbf{A}\right)^{-1}. \tag{37}$$

Case 3. Weighted Variable Range, Variable Variance Collection

For this case we allow both ranges and variances to vary. Furthermore, we will weight the measurements according to Eq. (24). If we implement the weighting as given in Eq. (24), with Eq. (27), then Eq. (29) becomes

$$\frac{\mathbf{\Sigma}_s}{\sigma_{ref}^2} = \left|\mathbf{r}_{s,ref}\right|^2 \left(\mathbf{A}^T \mathbf{W} \mathbf{A}\right)^{-1}. \tag{38}$$

A tacit assumption here is that the various variances are known, or at least presumed known well enough. While choice of reference range $\left|\mathbf{r}_{s,ref}\right|$ can be somewhat arbitrary, because its value will cancel anyway in the final calculation of Eq. (38), the choice for σ_{ref}^2 is a little more problematic. We might choose σ_{ref}^2 to be equal to the variance of a particular measurement, or some function of all the variances from all the measurements. However, for purposes of evaluating the goodness of data from various data collection geometries and conditions, it might be just as easy, and perhaps ultimately more meaningful, to set $\sigma_{ref}^2 = 1$, in which case Eq. (38) becomes a calculation of the covariance matrix $\mathbf{\Sigma}_s$ itself.

2.4 Multilateration Examples

We now exemplify the previous discussion with some examples.

2.4.1 Straight-line Collection Geometry

Consider a collection geometry as illustrated in Figure 2, where seven SAR images are collected along a horizontal straight line. In addition, we are observing a scatterer at a true location with respect to a universal SRP of

$$\mathbf{s} = \begin{bmatrix} 3 & 2 & 1 \end{bmatrix}^T \text{ m.} \tag{39}$$

However, the matrix $\mathbf{A}$ for this geometry is identified as

$$\mathbf{A} \approx \begin{bmatrix} -9396.9 & -6264.6 & -3132.3 & 0 & 3132.3 & 6264.6 & 9396.9 \\ 9396.9 & 9396.9 & 9396.9 & 9396.9 & 9396.9 & 9396.9 & 9396.9 \\ 3420.2 & 3420.2 & 3420.2 & 3420.2 & 3420.2 & 3420.2 & 3420.2 \end{bmatrix}^T, \tag{40}$$

which clearly has a rank of only two. Consequently $\mathbf{A}^T\mathbf{A}$ is singular, its inverse doesn't exist, and Eq. (14) cannot be calculated. This renders this geometry as unsuitable for 3-D geolocation using range-only measurements.

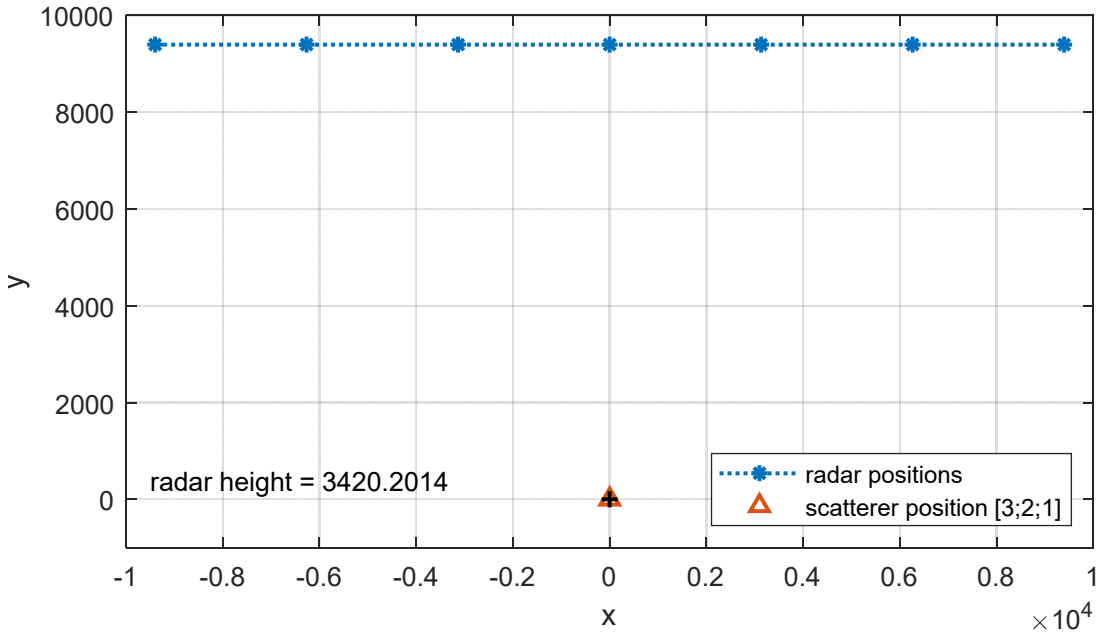

Figure 2. Straight-line data collection geometry. All numerical values in meters.

2.4.2 Circular Orbit Arc

Now consider the collection geometry of Figure 3, where the SAR images are collected along a constant-radius (from the SRP) circular orbiting arc. As before, we are observing a scatterer at a true location with respect to a universal SRP of

$$\mathbf{s} = \begin{bmatrix} 3 & 2 & 1 \end{bmatrix}^T \text{ m.} \tag{41}$$

For this geometry, **A** is of full rank, and exhibits a condition number of about 22.‡ With no measurement errors, we may use Eq. (14) to calculate a solution that exactly yields the scatterer coordinates in Eq. (41). We may furthermore calculate the DOP numbers as

$$\mathbf{d}_{DOP} \approx \begin{bmatrix} 0.8324 & 3.5789 & 8.6092 \end{bmatrix}^T. \tag{42}$$

This suggests that for this geometry, estimating the scatterer height (z component) from noisy measurements will amplify the standard deviation by about 8.6, which isn't too bad at all.

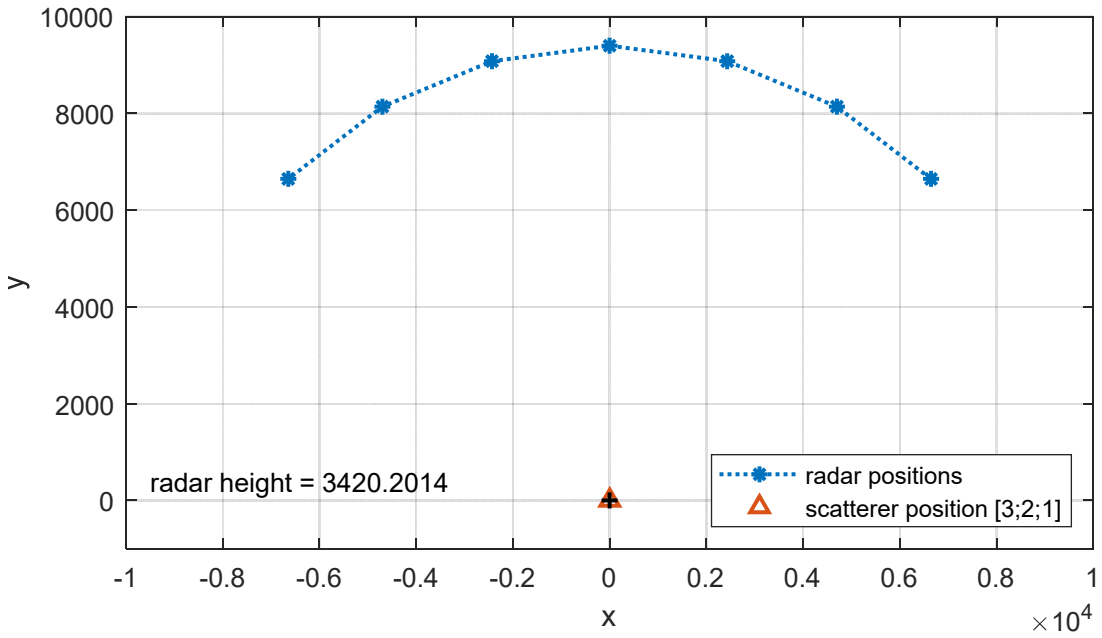

Figure 3. Circular Orbit Arc collection geometry. All numerical values in meters.

‡ As calculated by the Matlab 2-norm condition number with respect to inversion function, cond().

We may illustrate sensitivity to measurement noise by adding a small amount of random noise to all measurements $\left|\mathbf{r}_{s,i}\right|$. We will presume to add independent zero-mean Gaussian distributed noise with a standard deviation of 0.1 m. Table 1 details some sample results from a set of independent experimental simulations. Note that as the DOP values suggest, small errors in range measurements yield relatively small errors in estimated scatterer geolocation.

Table 1. Sample results from a set of independent experimental simulations where noise with a standard deviation of 0.1 m was added to the range measurements. Scatterer true location is at $\mathbf{s} = \begin{bmatrix} 3 & 2 & 1 \end{bmatrix}^T$.

Simulation	*Estimated Scatterer Geolocation (m)*
1	[2.9289 1.8348 1.4177] T
2	[2.9610 1.7169 1.7289] T
3	[3.1101 2.1985 0.4718] T
4	[2.9925 2.3402 0.2849] T
5	[3.0252 1.7686 1.3758] T

We can improve the DOP values somewhat by collecting additional range measurements. For example, if instead of collecting only 7 range samples along the quarter-circle arc in Figure 3, we collect 77 range samples, then the DOP values are improved to

$$\mathbf{d}_{DOP} \approx \begin{bmatrix} 0.2812 & 1.3447 & 3.3336 \end{bmatrix}^T . \tag{43}$$

Let us now consider that instead of a random zero-mean error added to the measurements $\left|\mathbf{r}_{s,i}\right|$, we instead add a bias of 3 m to all measurements $\left|\mathbf{r}_{s,i}\right|$. Such an error is in the neighborhood of what an atmospheric propagation delay might cause at these ranges. The result is an estimated scatterer geolocation of

$$\hat{\mathbf{s}} = \begin{bmatrix} 3.0009 & 2.0006 & -7.7638 \end{bmatrix}^T \text{ m.} \tag{44}$$

Note that for this geometry, a measurement bias in $\left|\mathbf{r}_{s,i}\right|$ yields primarily an error in geolocation height. A positive bias pushes the estimated height downward.

“What's right is what's left if you do everything else wrong.”
-- Robin Williams

3 Multilateration with a Range Bias

Heretofore we have assumed that the radar can make reasonably accurate "true range" measurements $\left|\mathbf{r}_{s,i}\right|$, and tacitly assumed that any error is zero mean. For a radar system to optimally calculate true range means that it needs to be well calibrated, and compensate for the actual velocity of propagation in the atmosphere. Falling short in either of these will impart a bias to the range error. This error bias may have elements that are common to all range measurements, and some that vary somewhat with collection geometry. Since we might expect a high degree of correlation in this error bias across our ranging samples (that's kind of what "bias" means), we might consider estimating this bias from the data itself, and compensating for this estimate in our estimation of scattering location *S*.

Let us now consider an error bias in the radar's measurement of range. Accordingly, we define

$$\begin{aligned}
&\left|\mathbf{r}_{s,true,i}\right| = \text{magnitude of the true geometric range from } S \text{ to APC}_i, \\
&\left|\mathbf{r}_{s,meas,i}\right| = \text{magnitude of radar's estimate or measure of the true range, and} \\
&r_{bias,i} = \text{bias in } \left|\mathbf{r}_{s,meas,i}\right|.
\end{aligned} \tag{45}$$

We might consider that the bias is a mean error, namely

$$r_{bias,i} = E\left\{\left|\mathbf{r}_{s,meas,i}\right| - \left|\mathbf{r}_{s,true,i}\right|\right\}. \tag{46}$$

In the absence of any statistical variations, we might simply assume

$$r_{bias,i} = \left|\mathbf{r}_{s,meas,i}\right| - \left|\mathbf{r}_{s,true,i}\right|. \tag{47}$$

In this case, Eq. (6) becomes

$$\mathbf{r}_{c,i}{}^{T}\mathbf{s} = \frac{1}{2}\left(\left|\mathbf{r}_{c,i}\right|^2 - \left|\mathbf{r}_{s,true,i}\right|^2 + \left|\mathbf{s}\right|^2\right), \tag{48}$$

which can now be expanded to explicitly show the measured range and range bias as

$$\mathbf{r}_{c,i}{}^{T}\mathbf{s} = \frac{1}{2}\left(\left|\mathbf{r}_{c,i}\right|^2 - \left(\left|\mathbf{r}_{s,meas,i}\right|\right)^2 + \left|\mathbf{s}\right|^2 - r_{bias,i}^2\right) + \left|\mathbf{r}_{s,meas,i}\right| r_{bias,i}. \tag{49}$$

This might be rearranged to the equality

$$\mathbf{r}_{c,i}{}^{T}\mathbf{s} - \left|\mathbf{r}_{s,meas,i}\right| r_{bias,i} = \frac{1}{2}\left(\left|\mathbf{r}_{c,i}\right|^2 - \left(\left|\mathbf{r}_{s,meas,i}\right|\right)^2 + \left|\mathbf{s}\right|^2 - r_{bias,i}^2\right). \tag{50}$$

Since each measure $\left|\mathbf{r}_{s,meas,i}\right|$ may potentially have its own range bias $r_{bias,i}$, and we need to additionally estimate an unknown scattering location vector **s**, relying on range measurements alone will never allow us to have enough independent measurements to calculate all the unknowns we wish to calculate.

Consequently, for the following development we will assume a single range bias common to all range measurements $\left|\mathbf{r}_{s,meas,i}\right|$. If we assume that all the range biases are equal, then we can write a collection of range measurements as

$$\begin{bmatrix} \mathbf{r}_{c,1}{}^{T} & -\left|\mathbf{r}_{s,meas,1}\right| \\ \mathbf{r}_{c,2}{}^{T} & -\left|\mathbf{r}_{s,meas,2}\right| \\ \vdots & \vdots \\ \mathbf{r}_{c,M}{}^{T} & -\left|\mathbf{r}_{s,meas,M}\right| \end{bmatrix} \begin{bmatrix} \mathbf{s} \\ r_{bias} \end{bmatrix} = \begin{bmatrix} \frac{1}{2}\left(\left|\mathbf{r}_{c,1}\right|^2 - \left(\left|\mathbf{r}_{s,meas,1}\right|\right)^2 + \left|\mathbf{s}\right|^2 - r_{bias}^2 \right) \\ \frac{1}{2}\left(\left|\mathbf{r}_{c,2}\right|^2 - \left(\left|\mathbf{r}_{s,meas,2}\right|\right)^2 + \left|\mathbf{s}\right|^2 - r_{bias}^2 \right) \\ \vdots \\ \frac{1}{2}\left(\left|\mathbf{r}_{c,M}\right|^2 - \left(\left|\mathbf{r}_{s,meas,M}\right|\right)^2 + \left|\mathbf{s}\right|^2 - r_{bias}^2 \right) \end{bmatrix}, \tag{51}$$

where

$$r_{bias,i} = r_{bias} \text{ = common constant, albeit unknown.} \tag{52}$$

This is of course of the well-known form

$$\mathbf{A}\mathbf{x} = \mathbf{b}, \tag{53}$$

where the matrix and vector elements are now

$$\mathbf{x} = \begin{bmatrix} \mathbf{s} \\ r_{bias} \end{bmatrix} = 4\times 1 \text{ column vector,}$$

$$\mathbf{A} = \begin{bmatrix} \mathbf{r}_{c,1}{}^{T} & -\left|\mathbf{r}_{s,meas,1}\right| \\ \mathbf{r}_{c,2}{}^{T} & -\left|\mathbf{r}_{s,meas,2}\right| \\ \vdots & \vdots \\ \mathbf{r}_{c,M}{}^{T} & -\left|\mathbf{r}_{s,meas,M}\right| \end{bmatrix} = \text{M}\times 4 \text{ matrix, and}$$

$$\mathbf{b} = \begin{bmatrix} \frac{1}{2}\left(\left|\mathbf{r}_{c,1}\right|^2 - \left(\left|\mathbf{r}_{s,meas,1}\right|\right)^2 + \left|\mathbf{s}\right|^2 - r_{bias}^2 \right) \\ \frac{1}{2}\left(\left|\mathbf{r}_{c,2}\right|^2 - \left(\left|\mathbf{r}_{s,meas,2}\right|\right)^2 + \left|\mathbf{s}\right|^2 - r_{bias}^2 \right) \\ \vdots \\ \frac{1}{2}\left(\left|\mathbf{r}_{c,M}\right|^2 - \left(\left|\mathbf{r}_{s,meas,M}\right|\right)^2 + \left|\mathbf{s}\right|^2 - r_{bias}^2 \right) \end{bmatrix} = \text{M}\times 1 \text{ column vector.} \tag{54}$$

With this new parameter to estimate, for a solution, we now require at least four independent measurements, that is $M \geq 4$.

For precisely four independent measurements, if **A** is full rank, we may calculate

$$\hat{\mathbf{x}} = \mathbf{A}^{-1}\mathbf{b}. \tag{55}$$

If we have more than four measurements, with **A** being full rank, we may calculate a least-squares solution as

$$\hat{\mathbf{x}} = \left(\mathbf{A}^T\mathbf{A}\right)^{-1}\mathbf{A}^T\mathbf{b}. \tag{56}$$

And finally, if wish to weight the input measurements, then we may calculate

$$\hat{\mathbf{x}} = \left(\mathbf{A}^T\mathbf{W}\mathbf{A}\right)^{-1}\mathbf{A}^T\mathbf{W}\mathbf{b}, \tag{57}$$

where often **W** is chosen to be a diagonal matrix with diagonal elements that are the inverse of the variances of the inputs in, or elements of, the **b** vector.

The $\hat{\mathbf{x}}$ vector contains estimates of its constituents

$$\hat{\mathbf{x}} = \begin{bmatrix} \hat{\mathbf{s}} \\ \hat{r}_{bias} \end{bmatrix}. \tag{58}$$

Some Comments on Calculating a Solution

Similar to the comments on solving Eq. (10), we comment on several issues of potential concern while calculating a solution to Eq. (53).

- First, as with Eq. (10), we note that our **b** vector still contains $|\mathbf{s}|^2$, but now also contains r_{bias}^2, both functions of the things we are trying to calculate. The same options previously discussed still apply here, namely ignoring the issue, using an approximation, using iteration in calculating a solution, or using elimination methods.

- Second, we are still presuming that the radar can reasonably accurately measure range $|\mathbf{r}_{s,i}|$, at least to within some hopefully small common range bias. We observe anecdotally that approximate solutions and iterative techniques usually work best the closer we begin to the final solution. Consequently, if we have "better" models for atmospheric propagation, then we should use them in compensating any "known" or "approximately known" structural biases in $|\mathbf{r}_{s,i}|$ perhaps due to variations in range, prior

to engaging any of the calculation Eq. (55) through Eq. (57). We may then leave any bias estimation for estimating a common residual bias error.

- Third, we continue to presume that our navigation subsystem can reasonably accurately measure radar position $\mathbf{r}_{a,i}$, and by extension $\mathbf{r}_{c,i}$.

- Fourth, it is still true that to use any of the calculations Eq. (55) through Eq. (57), the matrix **A** must be of full rank. Furthermore, we really desire that $\left(\mathbf{A}^T\mathbf{A}\right)$ is well conditioned so that small errors in **b** don't blow up. This means that we still cannot tolerate colinear or coplanar radar collection geometries.

  However, the addition of a fourth parameter to estimate, in this case r_{bias}, provides us with another column in matrix **A**, and hence another opportunity for linear dependence. That is, the first three columns of **A** that are associated with position vector **s** might still be linearly independent, but we also require the fourth column to be linearly independent of the others as well. Because we want to estimate four parameters now, we need the rank of matrix **A** to be four. A rank of three is no longer good enough.

  This additional constraint on the fourth column of **A**, because we want to estimate r_{bias}, places addition constraints on radar collection geometries. This means that data collection geometries that are good enough for otherwise estimating only **s**, may not be good enough for estimating both **s** and r_{bias} together. For example, a radar exhibiting a constant altitude and constant range circular orbit around some scattering location will render a range bias as indistinguishable from a height error, as shown in the example of Section 2.4.2. Even an approximate circular orbit can be expected to yield large errors in r_{bias} and/or height estimation.

  The bottom line is that if we want to estimate range bias from ranging data in addition to 3D scattering location **s**, then collecting that data with a constant altitude and constant range circular orbit is generally a no-no.

  One exception to this generalization might be if we had independent measurements or other information of either r_{bias} or scatterer height that are uncorrelated with the other, which would need to be included in the **A** matrix.

3.1 Dilution of Precision (DOP)

The DOP calculations are essentially the same as in Section 2.3, namely they are derived from the diagonal of a normalized covariance matrix

$$\frac{\mathbf{\Sigma}_s}{\sigma_{ref}^2} = \left|\mathbf{r}_{s,ref}\right|^2 \mathbf{C}\,\mathbf{K}\,\mathbf{C}^T, \tag{59}$$

where in the general sense

$$\mathbf{C} = \left(\mathbf{A}^T\mathbf{W}\mathbf{A}\right)^{-1}\mathbf{A}^T\mathbf{W}, \tag{60}$$

and

$$\mathbf{K} = \mathrm{diag}\left(\left[\left(\frac{\left|\mathbf{r}_{s,1}\right|^2\sigma_{s,1}^2}{\left|\mathbf{r}_{s,ref}\right|^2\sigma_{ref}^2}\right)\ \left(\frac{\left|\mathbf{r}_{s,2}\right|^2\sigma_{s,2}^2}{\left|\mathbf{r}_{s,ref}\right|^2\sigma_{ref}^2}\right)\ \cdots\ \left(\frac{\left|\mathbf{r}_{s,M}\right|^2\sigma_{s,M}^2}{\left|\mathbf{r}_{s,ref}\right|^2\sigma_{ref}^2}\right)\right]\right). \tag{61}$$

Specifically, the DOP values are

$$\mathbf{d}_{DOP} = \mathrm{diag}\left(\frac{\mathbf{\Sigma}_s}{\sigma_{ref}^2}\right)^{1/2}, \tag{62}$$

understanding that the square-root operation is on elements of the diagonal. The difference now is that $\mathbf{d}_{DOP}$ is a 4-element vector, that includes the DOP for geolocation estimate **s**, and now also the DOP for the bias estimate r_{bias}.

Depending on the nature of $\left|\mathbf{r}_{s,i}\right|$ and $\sigma_{s,i}^2$, we might choose $\mathbf{W} = \mathbf{I}$, or perhaps a weighted least-squares solution with $\mathbf{W} = \mathbf{K}^{-1}$.

Comments

Although we have added the estimation of a common range bias, the underlying measurements from which we derive these estimates are the same. That is, the **K** matrix in this section is the same as for the DOP calculations in Section 2.3.

3.2 Multilateration Examples

We now exemplify the previous discussion with some examples.

3.2.1 Circular Orbit Arc

We now revisit the example in Section 2.4.2, where the SAR images are collected along a constant-radius (from the SRP) circular orbiting arc, as illustrated again in Figure 4. As before, we are observing a scatterer at a true location with respect to a universal SRP, but now also with a fixed true range bias, of

$$\mathbf{s} = \begin{bmatrix} 3 & 2 & 1 \end{bmatrix}^T \text{ m, and}$$
$$r_{bias} = 3 \text{ m.} \tag{63}$$

For this geometry, although matrix **A** is technically of full rank, it exhibits an incredibly poor condition number of about 10^9. With no measurement errors, we may use Eq. (56) and Eq. (58) to calculate a solution that yields the estimates[§]

$$\hat{\mathbf{s}} = \begin{bmatrix} 3.0009 & 2.0006 & -9.6778 \end{bmatrix}^T \text{ m, and}$$
$$\hat{r}_{bias} = -0.71145 \text{ m.} \tag{64}$$

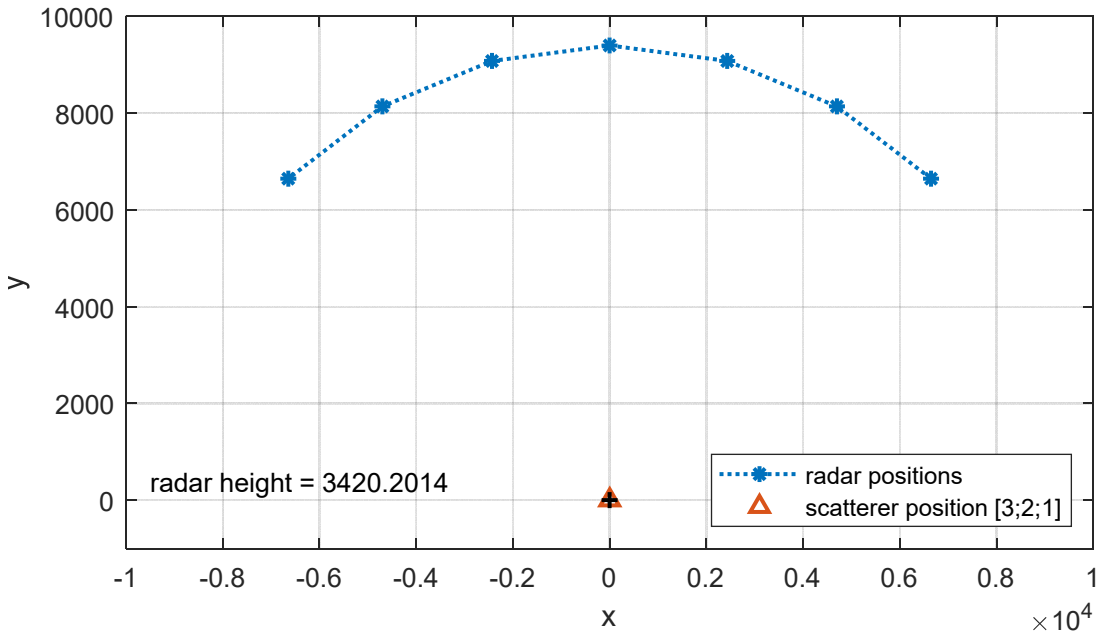

Figure 4. Circular Orbit Arc collection geometry. All numerical values in meters.

[§] Calcluations using Matlab double-precision arithmetic.

Observe that the error in the calculated range bias is about 3.7 m, which is worse than if we had just ignored it entirely. Furthermore, the error in scatterer height estimation is almost 11 m, again worse than if we had just ignored the range bias. So, by attempting to estimate the range bias, we made our geolocation estimation worse, not better.

Note that in spite of essentially "perfect" measurements (within the limits of double-precision arithmetic) the results in Eq. (64) contain significant errors. Even reducing the true range bias to zero, but still allowing for its estimation nonetheless, will generate similarly large estimation errors.

Had the true target position been exactly at the center of the orbit, then the rank of matrix $\mathbf{A}$ would have been only 3, rendering $\left(\mathbf{A}^T\mathbf{A}\right)$ as singular, and impossible to invert at all, and hence impossible with which to calculate a geolocation solution.

We may gain further insight into the reason for poor performance by calculating the DOP numbers for our example to be

$$\mathbf{d}_{DOP} \approx \begin{bmatrix} 1489 & 992 & 1.45\times10^{7} & 4.96\times10^{6} \end{bmatrix}^T . \tag{65}$$

The first three entries are associated with $\hat{\mathbf{s}}$, and the fourth describes $\hat{r}_{bias}$. We observe from this that we might expect even very small errors, perhaps even mere quantization errors, to be greatly amplified in the calculation of a solution, especially for height estimation and range bias estimation.

We may illustrate sensitivity to measurement noise by adding a small amount of random noise to all measurements $\left|\mathbf{r}_{s,i}\right|$. We will presume to again add independent zero-mean Gaussian distributed noise with a standard deviation of 0.1 m. Unfortunately, the errors are so amplified that the iterative technique used to calculate $\hat{\mathbf{x}}$, and hence $\hat{\mathbf{s}}$ and $\hat{r}_{bias}$, won't even converge to a solution.

The net effect is that by adding another degree of freedom to our problem so that we might estimate $\hat{r}_{bias}$, in fact increases our DOP values so that we become super sensitive to even small errors, and makes our estimates so much worse as to become meaningless and unusable.

So, more isn't always better.

We summarize by restating that if we are estimating range biases in addition to scatterer geolocation, then collecting range data with a constant altitude and constant range circular orbit is a poor choice.[**]

[**] We remind the reader that this is for range-only data, without any other independent data.

3.2.2 Spiral Arc

Now consider a group of SAR images collected along a constant-altitude spiral arc illustrated in Figure 5. Both range and grazing angle vary with each image.

As before, we are observing a scatterer at a true location with respect to a universal SRP, but now also with a fixed true range bias, of

$$\mathbf{s} = \begin{bmatrix} 3 & 2 & 1 \end{bmatrix}^T \text{ m, and}$$
$$r_{bias} = 3 \text{ m.} \tag{66}$$

For this geometry, matrix **A** is full rank, and exhibits a condition number of about 194. With no measurement errors, we may use Eq. (56) and Eq. (58) to calculate a solution that yields the perfect estimates[††]

$$\hat{\mathbf{s}} = \begin{bmatrix} 3.0000 & 2.0000 & 1.0000 \end{bmatrix}^T \text{ m, and}$$
$$\hat{r}_{bias} = 3 \text{ m.} \tag{67}$$

This is a substantially improved result from the previous constant-radius circular orbiting arc.

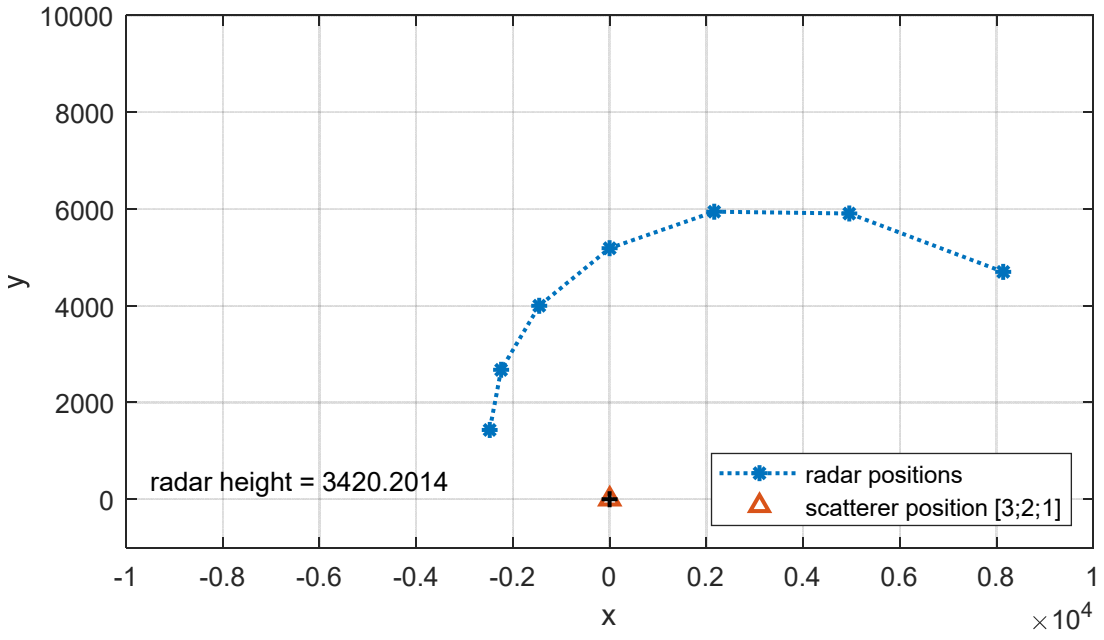

Figure 5. Spiral Arc collection geometry. All numerical values in meters.

[††] Calcluations using Matlab double-precision arithmetic.

We calculate the DOP numbers to be

$$\mathbf{d}_{DOP} \approx \begin{bmatrix} 12.9143 & 4.5254 & 45.2824 & 28.3273 \end{bmatrix}^T , \tag{68}$$

which is also much improved from the previous example. We recall that the first three entries are associated with $\hat{\mathbf{s}}$, and the fourth describes $\hat{r}_{bias}$.

We may illustrate sensitivity to measurement noise by adding a small amount of random noise to all measurements $\left|\mathbf{r}_{s,i}\right|$, again presuming to add independent zero-mean Gaussian distributed noise with a standard deviation of 0.1 m. Sample results are given in Table 2. Note that as the DOP values suggest, small errors in range measurements are multiplied to larger errors in estimated scatterer geolocation. Nevertheless, this is much improved from the previous example.

Table 2. Sample results from a set of independent experimental simulations where noise with a standard deviation of 0.1 m was added to the range measurements. Scatterer true location is at $\mathbf{s} = \begin{bmatrix} 3 & 2 & 1 \end{bmatrix}^T$ with a constant range bias of 3 m.

Simulation	*Estimated Scatterer Geolocation (m)*	*Estimated Range Bias (m)*
1	[3.1842 1.9528 1.7831] T	3.4266
2	[3.6305 2.3184 3.1353] T	4.4048
3	[2.5120 2.1401 -0.7543] T	1.9692
4	[5.4104 2.4614 9.4918] T	8.1420
5	[2.9815 1.7387 0.5437] T	2.5614

We observe from all this that for range-only measurements, the constant-altitude spiral arc is a superior geometry over the constant-range circular orbit arc.

We also observe that the estimated range bias in the simulation examples of Table 2 vary over a span of about 6 m; from about 2 m to about 8 m. We opine that for a well-calibrated radar, and with even a rudimentary correction for atmospheric propagation, that such a large span is highly unlikely. This begs the question "Can we incorporate some additional information that might constrain the range bias estimate, and thereby improve geolocation of the scatterer as well?" The answer is "yes."

“Sometimes the road less traveled is less traveled for a reason.”
-- Jerry Seinfeld

4 Multilateration with a Tethered Range Bias

In the previous section we examined estimating a scatterer's geolocation in the presence of a range measurement bias error common to all range measurements. It became clear that attempts to estimate the range bias in addition to scatterer geolocation encountered some difficulties, and further limited suitable data collection geometries, often increasing sensitivities to ranging errors and increasing DOPs to unusable conditions.

The treatment in previous section allowed for an unconstrained floating of range bias to ultimately minimize overall squared error. However, this is somewhat unrealistic in many situations where we can reasonably bound range bias due to factors such as atmospheric propagation. Consequently, it makes sense to incorporate this additional information into the geolocation estimation process.

As in the previous section, we will continue with the definitions of Eq. (45) through Eq. (50), and also continue to assume a single range bias common to all range measurements $\left|\mathbf{r}_{s,meas,i}\right|$, where

$$r_{bias,i} = r_{bias} = \text{constant, albeit unknown.} \tag{69}$$

In this section, however, we will presume to incorporate an initial guess at the range bias in the form of a tether value, and introduce

$$r_{bias,tether,i} = \text{presumed best guess of the residual bias in } \left|\mathbf{r}_{s,meas,i}\right|. \tag{70}$$

The intent is to substantially restrain, but still allow some elasticity, to the final range bias estimate. We will assume a single common tether value for all range measures, that is

$$r_{bias,tether,i} = r_{bias,tether} = \text{constant.} \tag{71}$$

We continue to structure our matrix equation as

$$\mathbf{A}\mathbf{x} = \mathbf{b}, \tag{72}$$

where, as before, we wish to solve for

$$\mathbf{x} = \begin{bmatrix} \mathbf{s} \\ r_{bias} \end{bmatrix} = 4\times 1 \text{ column vector.} \tag{73}$$

However, we now add to matrix **A** and vector **b** an additional condition, so that they now become

$$\mathbf{A} = \begin{bmatrix} \mathbf{r}_{c,1}{}^{T} & -\left|\mathbf{r}_{s,meas,1}\right| \\ \mathbf{r}_{c,2}{}^{T} & -\left|\mathbf{r}_{s,meas,2}\right| \\ \vdots & \vdots \\ \mathbf{r}_{c,M}{}^{T} & -\left|\mathbf{r}_{s,meas,M}\right| \\ \begin{bmatrix} 0 & 0 & 0 \end{bmatrix} & 1 \end{bmatrix} = (\mathrm{M}+1)\times 4 \text{ matrix, and}$$

$$\mathbf{b} = \begin{bmatrix} \frac{1}{2}\left(\left|\mathbf{r}_{c,1}\right|^2 - \left(\left|\mathbf{r}_{s,meas,1}\right| \right)^2 + \left|\mathbf{s}\right|^2 - r_{bias}^2 \right) \\ \frac{1}{2}\left(\left|\mathbf{r}_{c,2}\right|^2 - \left(\left|\mathbf{r}_{s,meas,2}\right| \right)^2 + \left|\mathbf{s}\right|^2 - r_{bias}^2 \right) \\ \vdots \\ \frac{1}{2}\left(\left|\mathbf{r}_{c,M}\right|^2 - \left(\left|\mathbf{r}_{s,meas,M}\right| \right)^2 + \left|\mathbf{s}\right|^2 - r_{bias}^2 \right) \\ r_{bias,tether} \end{bmatrix} = (\mathrm{M}+1)\times 1 \text{ column vector.} \quad (74)$$

This construct will attempt to calculate $r_{bias} = r_{bias,tether}$ in the least-squares sense. Consequently, we are tethering our estimate for r_{bias} to a presumed value $r_{bias,tether}$. The fact that we are allowing some departure from this value due to minimizing the overall squared error calculation for **x** provides some elasticity to matching $r_{bias,tether}$ precisely.

A question remains "How much elasticity should we give to force $r_{bias} = r_{bias,tether}$?" We can address this with a weighted least-squares solution, placing greater weight onto this relationship. The question then becomes "How do we choose a weighting?"

Comments

While in this section we are tethering range bias, there is no overt reason that the same concept of tethering can't be applied to other parameters, say, any of the geolocation parameters. Any information about any of our parameters, from any other source, might be incorporated in some fashion into the matrix equation, to help calculate a hopefully improved geolocation solution.

4.1 Weighted Least Squares Solution

Following the development in Section 2.2, we may calculate the covariance matrix for this new **b** to be

$$\boldsymbol{\Sigma}_b = \mathrm{diag}\left(\left[\left(\left|\mathbf{r}_{s,1}\right|^2 \sigma_{s,1}^2\right) \;\; \left(\left|\mathbf{r}_{s,2}\right|^2 \sigma_{s,2}^2\right) \;\; \cdots \;\; \left(\left|\mathbf{r}_{s,M}\right|^2 \sigma_{s,M}^2\right) \;\; \sigma_{bias,tether}^2\right]\right), \tag{75}$$

where the new variance entry is

$$\sigma_{bias,tether}^2 = \text{variance we allow in matching } r_{bias} \text{ to } r_{bias,tether}. \tag{76}$$

We may again write the covariance matrix $\boldsymbol{\Sigma}_b$ as

$$\boldsymbol{\Sigma}_b = \left|\mathbf{r}_{s,ref}\right|^2 \sigma_{ref}^2 \mathbf{K}, \tag{77}$$

where now the **K** matrix becomes

$$\mathbf{K} = \mathrm{diag}\left(\left[\left(\frac{\left|\mathbf{r}_{s,1}\right|^2 \sigma_{s,1}^2}{\left|\mathbf{r}_{s,ref}\right|^2 \sigma_{ref}^2}\right) \;\; \left(\frac{\left|\mathbf{r}_{s,2}\right|^2 \sigma_{s,2}^2}{\left|\mathbf{r}_{s,ref}\right|^2 \sigma_{ref}^2}\right) \;\; \cdots \;\; \left(\frac{\left|\mathbf{r}_{s,M}\right|^2 \sigma_{s,M}^2}{\left|\mathbf{r}_{s,ref}\right|^2 \sigma_{ref}^2}\right) \;\; \left(\frac{\sigma_{bias,tether}^2}{\left|\mathbf{r}_{s,ref}\right|^2 \sigma_{ref}^2}\right)\right]\right). \tag{78}$$

Consequently, we may choose a weighting matrix for a weighted least-squares solution to be

$$\mathbf{W} = \mathbf{K}^{-1}. \tag{79}$$

Using this we may calculate the weighted least-squares solution to be

$$\hat{\mathbf{x}} = \left(\mathbf{A}^T \mathbf{W} \mathbf{A}\right)^{-1} \mathbf{A}^T \mathbf{W} \mathbf{b}. \tag{80}$$

We expect that typically the variance in the bias is substantially less than the range-scaled variance of the range measurements, that is

$$\sigma_{bias,tether}^2 << \left|\mathbf{r}_{s,i}\right|^2 \sigma_{s,i}^2. \tag{81}$$

Because its magnitude is constrained in Eq. (81), the contribution of $\sigma_{bias,tether}^2$ in Eq. (78) is substantially subdued. Consequently, the weighting matrix selected in Eq. (79) must amplify its effect in the final solution. This implies that we may expect that a substantially enhanced weighting will be applied towards encouraging $r_{bias} = r_{bias,tether}$.

We note that this is related to constrained least-squares techniques which can be found in various references, for example in a text by Van Trees.[11]

4.2 Dilution of Precision (DOP)

The DOP calculations are essentially the same as in previous sections, namely they are derived from the diagonal of a normalized covariance matrix

$$\frac{\mathbf{\Sigma}_s}{\sigma_{ref}^2} = \left|\mathbf{r}_{s,ref}\right|^2 \mathbf{C}\,\mathbf{K}\,\mathbf{C}^T , \tag{82}$$

where in the general sense

$$\mathbf{C} = \left(\mathbf{A}^T\mathbf{W}\mathbf{A}\right)^{-1}\mathbf{A}^T\mathbf{W} , \tag{83}$$

and, repeating Eq. (78), we have

$$\mathbf{K} = \mathrm{diag}\left(\left[\left(\frac{\left|\mathbf{r}_{s,1}\right|^2\sigma_{s,1}^2}{\left|\mathbf{r}_{s,ref}\right|^2\sigma_{ref}^2}\right)\ \left(\frac{\left|\mathbf{r}_{s,2}\right|^2\sigma_{s,2}^2}{\left|\mathbf{r}_{s,ref}\right|^2\sigma_{ref}^2}\right)\ \cdots\ \left(\frac{\left|\mathbf{r}_{s,M}\right|^2\sigma_{s,M}^2}{\left|\mathbf{r}_{s,ref}\right|^2\sigma_{ref}^2}\right)\ \left(\frac{\sigma_{bias,tether}^2}{\left|\mathbf{r}_{s,ref}\right|^2\sigma_{ref}^2}\right)\right]\right). \tag{84}$$

Specifically, the DOP values are

$$\mathbf{d}_{DOP} = \mathrm{diag}\left(\frac{\mathbf{\Sigma}_s}{\sigma_{ref}^2}\right)^{1/2} , \tag{85}$$

understanding that the square-root operation is on elements of the diagonal. We observe that $\mathbf{d}_{DOP}$ is still a 4-element vector, that includes the DOP for geolocation estimate **s**, and also the DOP for the bias estimate r_{bias}.

Comments

Augmenting and contrasting with the comments at the end of Section 2.3, we still have a **K** matrix for which the range measurement biases $\sigma_{s,i}^2$ might still be assumed to be essentially equal. However, the **K** matrix in Eq. (84) now also explicitly contains the variance of the tether bias itself, $\sigma_{bias,tether}^2$. Since we ultimately expect any range bias variance due to the tether, to also be a constituent of the overall ranging error variance, it is reasonable to assume

$$\sigma_{bias,tether}^2 \approx \sigma_{s,i}^2 . \tag{86}$$

This means that σ_{ref}^2 may reasonably describe both of these.

4.3 Multilateration Examples

We now exemplify the previous discussion with some examples.

4.3.1 Circular Orbit Arc

We again revisit the example of a constant-radius (from the SRP) circular orbiting arc that was examined in Section 2.4.2 and Section 3.2.1. The geometry is again illustrated in Figure 6. As before, we are observing a scatterer at a true location with respect to a universal SRP, and a fixed true range bias, of

$$\mathbf{s} = \begin{bmatrix} 3 & 2 & 1 \end{bmatrix}^T \text{ m, and}$$
$$r_{bias} = 3 \text{ m.} \tag{87}$$

In addition, we will tether the range bias to

$$r_{bias,tether} = 3 \text{ m.} \tag{88}$$

For this geometry, matrix **A** is full rank, and exhibits a condition number of about 10^5. With no measurement errors, we may use a weighted least-squares calculation that yields perfect estimates of scatterer geolocation and range bias.

$$\hat{\mathbf{s}} = \begin{bmatrix} 3 & 2 & 1 \end{bmatrix}^T \text{ m, and}$$
$$\hat{r}_{bias} = 3 \text{ m.} \tag{89}$$

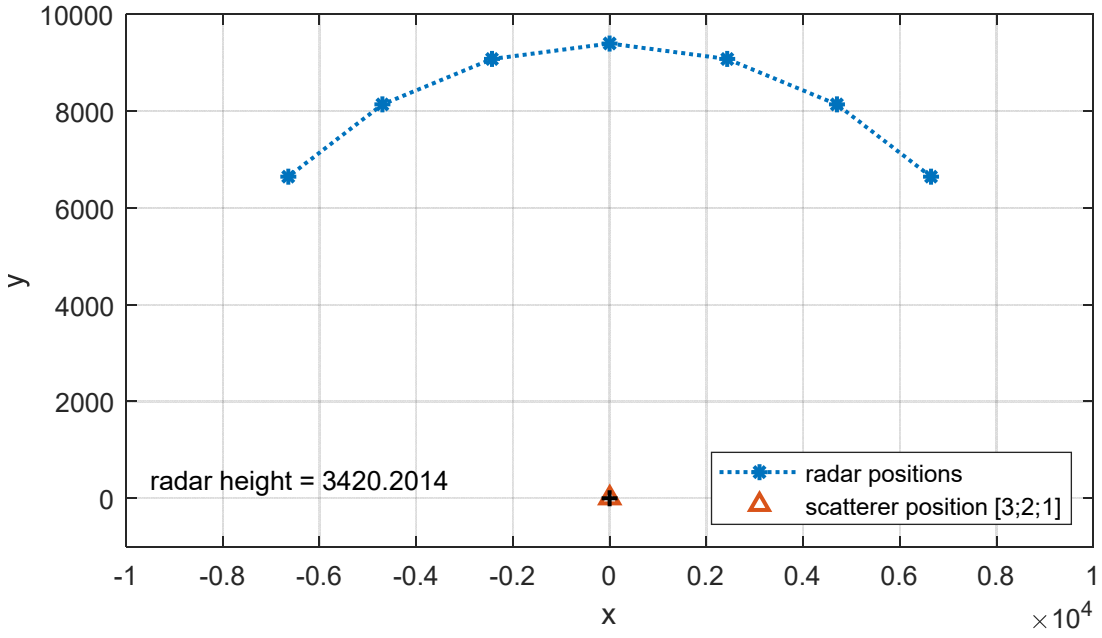

Figure 6. Circular Orbit Arc collection geometry. All numerical values in meters.

The weight matrix **W** was chosen using Eq. (78), with a somewhat arbitrary

$$\sigma^2_{bias,tether} = \sigma^2_{s,i} = \sigma^2_{ref} \,. \tag{90}$$

This substantially emphasizes the influence of our tether value $r_{bias,tether}$.

We calculate the corresponding DOP numbers to be a fairly reasonable

$$\mathbf{d}_{DOP} \approx \begin{bmatrix} 0.8326 & 3.5800 & 9.0948 & 1.0000 \end{bmatrix}^T . \tag{91}$$

We may illustrate sensitivity to measurement noise by adding a small amount of random noise to all measurements $\left|\mathbf{r}_{s,i}\right|$, again presuming to add independent zero-mean Gaussian distributed noise with a standard deviation of 0.1 m. In addition, we may assume some randomness to the true range bias, assumed to be Gaussian distributed around a mean of 3 m with a standard deviation of about 0.4 m. This is a reasonable approximation for atmospheric propagation variations. Sample simulation results are given in Table 3.

Note that as the DOP values suggest, small errors in range measurements net small errors in estimated scatterer geolocation. Nevertheless, this is much improved from the previous example.

Table 3. Sample results from a set of independent experimental simulations where noise with a standard deviation of 0.1 m was added to the range measurements, and range bias truth varied with a standard deviation of 0.4 m. Scatterer true location is at $\mathbf{s} = \begin{bmatrix} 3 & 2 & 1 \end{bmatrix}^T$ with tethered range bias of 3 m.

Simulation	*True Range Bias (m)*	*Estimated Scatterer Geolocation (m)*	*Estimated Range Bias (m)*
1	3.2868	[2.9786 1.1625 2.0155] T	3
2	2.6763	[2.8998 1.9155 2.2069] T	3
3	2.4035	[3.0561 2.0140 2.5716] T	3
4	3.1952	[2.8832 1.5743 1.5600] T	3
5	3.0863	[2.9811 1.8712 0.9480] T	3

The bottom line is that by tethering the range bias we overcome the otherwise extreme sensitivity to ranging errors so that this circular orbit collection geometry becomes useful again and in fact leads to fairly accurate geolocation performance.

4.3.2 Spiral Arc

We return now to the collection geometry of Section 3.2.2, where a group of SAR images was collected along a constant-altitude spiral arc, illustrated again in Figure 7. Recall that both range and grazing angle vary with each image.

As before, we are observing a scatterer at a true location with respect to a universal SRP, but with a fixed true range bias, of

$$\mathbf{s} = \begin{bmatrix} 3 & 2 & 1 \end{bmatrix}^T \text{ m, and}$$
$$r_{bias} = 3 \text{ m.} \tag{92}$$

In addition, we will tether the range bias to

$$r_{bias,tether} = 3 \text{ m.} \tag{93}$$

For this geometry, matrix **A** is full rank, and exhibits a condition number of about 194. With no measurement errors, we may use Eq. (56) and Eq. (58) to calculate a solution that yields the perfect estimates

$$\hat{\mathbf{s}} = \begin{bmatrix} 3.0000 & 2.0000 & 1.0000 \end{bmatrix}^T \text{ m, and}$$
$$\hat{r}_{bias} = 3 \text{ m.} \tag{94}$$

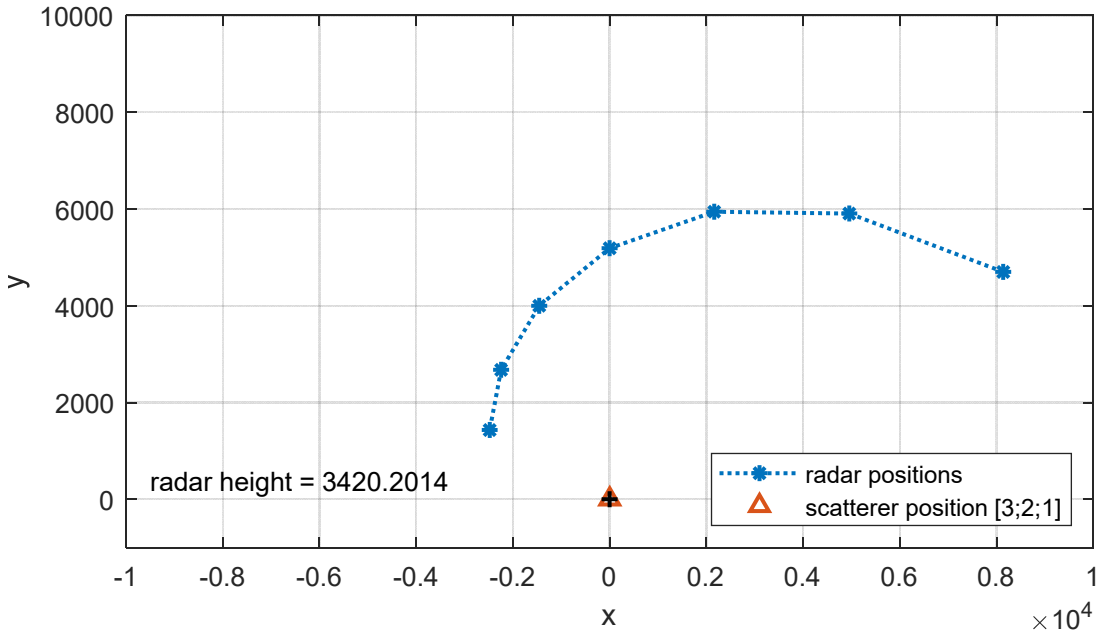

Figure 7. Spiral Arc collection geometry. All numerical values in meters.

We calculate the DOP numbers to be

$$\mathbf{d}_{DOP} \approx \begin{bmatrix} 1.2149 & 1.9909 & 2.7724 & 0.9993 \end{bmatrix}^T, \tag{95}$$

which is much improved from the example of Section 3.2.2. We recall that the first three entries are associated with $\hat{\mathbf{s}}$, and the fourth describes $\hat{r}_{bias}$.

We may illustrate sensitivity to measurement noise by adding a small amount of random noise to all measurements $\left|\mathbf{r}_{s,i}\right|$, again presuming to add independent zero-mean Gaussian distributed noise with a standard deviation of 0.1 m. In addition, we may assume some randomness to the true range bias, assumed to be Gaussian distributed around a mean of 3 m with a standard deviation of about 0.4 m. This is a reasonable approximation for atmospheric propagation variations. Sample results are given in Table 4. Note that as the DOP values suggest, small errors in range measurements are multiplied to not-too-much-larger errors in estimated scatterer geolocation.

Table 4. Sample results from a set of independent experimental simulations where noise with a standard deviation of 0.1 m was added to the range measurements, and range bias truth varied with a standard deviation of 0.4 m. Scatterer true location is at $\mathbf{s} = \begin{bmatrix} 3 & 2 & 1 \end{bmatrix}^T$ with a constant range bias of 3 m.

Simulation	*True Range Bias (m)*	*Estimated Scatterer Geolocation (m)*	*Estimated Range Bias (m)*
1	2.8981	[2.9376 2.0010 1.2490] T	3
2	2.4319	[3.3032 1.9752 2.0475] T	2.9983
3	3.1176	[3.1542 1.6169 1.2694] T	3.0109
4	3.3917	[2.6680 2.1849 0.1949] T	2.9934
5	3.1571	[3.0925 1.7626 0.9484] T	3.0019

We observe from all this that for range-only measurements, augmented by a tethered range bias, the constant-altitude spiral arc is still an excellent data collection geometry.

5 Differential Geolocation

Heretofore, in the previous sections, we have calculated an absolute geolocation for the scatterer of interest. In this section we deal with a relative location between two scatterers in the SAR images. For example, this might be useful for geolocating a point with respect to a fiducial reference point.

We investigate this problem by defining two scattering locations of interest, with vectors

$$\begin{aligned} \mathbf{s}_1 &= \text{location of scatterer } S_1, \text{ and} \\ \mathbf{s}_2 &= \text{location of scatterer } S_2. \end{aligned} \tag{96}$$

We will ignore any biases, and note that for each, the matrix equation is still

$$\begin{aligned} \mathbf{A}\,\mathbf{s}_1 &= \mathbf{b}_1, \text{ and} \\ \mathbf{A}\,\mathbf{s}_2 &= \mathbf{b}_2, \end{aligned} \tag{97}$$

where

$$\mathbf{A} = \begin{bmatrix} \mathbf{r}_{c,1}{}^T \\ \mathbf{r}_{c,2}{}^T \\ \vdots \\ \mathbf{r}_{c,M}{}^T \end{bmatrix} = M \times 3 \text{ square matrix,}$$

$$\mathbf{b}_1 = \begin{bmatrix} \frac{1}{2}\left(|\mathbf{r}_{c,1}|^2 - |\mathbf{r}_{s_1,1}|^2 + |\mathbf{s}_1|^2 \right) \\ \frac{1}{2}\left(|\mathbf{r}_{c,2}|^2 - |\mathbf{r}_{s_1,2}|^2 + |\mathbf{s}_1|^2 \right) \\ \vdots \\ \frac{1}{2}\left(|\mathbf{r}_{c,M}|^2 - |\mathbf{r}_{s_1,M}|^2 + |\mathbf{s}_1|^2 \right) \end{bmatrix} = M \times 1 \text{ column matrix for } S_1, \text{ and}$$

$$\mathbf{b}_2 = \begin{bmatrix} \frac{1}{2}\left(|\mathbf{r}_{c,1}|^2 - |\mathbf{r}_{s_2,1}|^2 + |\mathbf{s}_2|^2 \right) \\ \frac{1}{2}\left(|\mathbf{r}_{c,2}|^2 - |\mathbf{r}_{s_2,2}|^2 + |\mathbf{s}_2|^2 \right) \\ \vdots \\ \frac{1}{2}\left(|\mathbf{r}_{c,M}|^2 - |\mathbf{r}_{s_2,M}|^2 + |\mathbf{s}_2|^2 \right) \end{bmatrix} = M \times 1 \text{ column matrix for } S_2. \tag{98}$$

Taking the difference between the equations in Eq. (97) yields

$$\mathbf{A}\left(\mathbf{s}_2-\mathbf{s}_1\right)=\left(\mathbf{b}_2-\mathbf{b}_1\right). \tag{99}$$

We can write this more succinctly as

$$\mathbf{A}\,\mathbf{s}_\Delta=\mathbf{b}_\Delta, \tag{100}$$

where

$$\begin{aligned}&\mathbf{s}_\Delta=\mathbf{s}_2-\mathbf{s}_1, \text{ and}\\ &\mathbf{b}_\Delta=\mathbf{b}_2-\mathbf{b}_1.\end{aligned} \tag{101}$$

The vector $\mathbf{b}_\Delta$ may be expanded to

$$\mathbf{b}_\Delta=\begin{bmatrix}\frac{1}{2}\left(-\left|\mathbf{r}_{s_2,1}\right|^2+\left|\mathbf{r}_{s_1,1}\right|^2+\left|\mathbf{s}_2\right|^2-\left|\mathbf{s}_1\right|^2\right)\\ \frac{1}{2}\left(-\left|\mathbf{r}_{s_2,2}\right|^2+\left|\mathbf{r}_{s_1,2}\right|^2+\left|\mathbf{s}_2\right|^2-\left|\mathbf{s}_1\right|^2\right)\\ \vdots\\ \frac{1}{2}\left(-\left|\mathbf{r}_{s_2,M}\right|^2+\left|\mathbf{r}_{s_1,M}\right|^2+\left|\mathbf{s}_2\right|^2-\left|\mathbf{s}_1\right|^2\right)\end{bmatrix}. \tag{102}$$

We note that we may expand

$$\left|\mathbf{s}_2\right|^2-\left|\mathbf{s}_1\right|^2=\left|\mathbf{s}_\Delta\right|^2+2\mathbf{s}_\Delta\bullet\mathbf{s}_1. \tag{103}$$

This allows us to write

$$\mathbf{b}_\Delta=\begin{bmatrix}\frac{1}{2}\left(-\left|\mathbf{r}_{s_2,1}\right|^2+\left|\mathbf{r}_{s_1,1}\right|^2+\left|\mathbf{s}_\Delta\right|^2+2\mathbf{s}_1\bullet\mathbf{s}_\Delta\right)\\ \frac{1}{2}\left(-\left|\mathbf{r}_{s_2,2}\right|^2+\left|\mathbf{r}_{s_1,2}\right|^2+\left|\mathbf{s}_\Delta\right|^2+2\mathbf{s}_1\bullet\mathbf{s}_\Delta\right)\\ \vdots\\ \frac{1}{2}\left(-\left|\mathbf{r}_{s_2,M}\right|^2+\left|\mathbf{r}_{s_1,M}\right|^2+\left|\mathbf{s}_\Delta\right|^2+2\mathbf{s}_1\bullet\mathbf{s}_\Delta\right)\end{bmatrix}. \tag{104}$$

We then desire the solution which can be calculated as

$$\hat{\mathbf{s}}_\Delta=\left(\mathbf{A}^T\mathbf{A}\right)^{-1}\mathbf{A}^T\mathbf{b}_\Delta. \tag{105}$$

Some Comments on Calculating a Solution

Several points are worth noting.

- If $|\mathbf{s}_\Delta|$ is small compared to the radar ranges $|\mathbf{r}_{s_1,i}|$ and $|\mathbf{r}_{s_2,i}|$, then we would expect any range biases to be nearly identical, and hence irrelevant to the difference $|\mathbf{s}_\Delta|$.

- The presumption is that $\mathbf{s}_1$ is known. It is the reference or fiducial location to which other points are measured.

- We observe that $\mathbf{s}_\Delta$ also appears in our vector **b**. It is of course the thing we are trying to calculate. This suggests that we may wish to consider any of the techniques discussed in the comments after Eq. (10), including perhaps an iterative technique, for its calculation.

- We note that if $|\mathbf{s}_1| = 0$, then we expect $|\mathbf{r}_{s_1,i}| = |\mathbf{r}_{c,i}|$, and $\mathbf{b}_\Delta$ in Eq. (104) looks very much like $\mathbf{b}_2$ in Eq. (98), and our solution becomes $\mathbf{s}_\Delta = \mathbf{s}_2$. One might wonder how this then differs from the algorithm discussed in Section 2.1.

  The subtle but very important distinction is that in Section 2.1 the value $|\mathbf{r}_{c,i}|$ in the **b** vector is derived from the radar's navigation subsystem, whereas in this section, $|\mathbf{r}_{s_1,i}|$ is derived from a radar's ranging measurement. While in a perfect world they should be equal, in the decidedly imperfect world we have they are not, with one containing motion measurement errors, and the other containing biases and errors due to propagation; essentially the same errors as $|\mathbf{r}_{s_2,i}|$, as discussed above.

- A 3-D solution to Eq. (105) requires at least 3 SAR images.

"The New England Journal of Medicine reports that 9 out of 10 doctors agree that 1 out of 10 doctors is an idiot."
-- Jay Leno

6 Differential Ranging

In earlier developments we examined an $\mathbf{Ax} = \mathbf{b}$ matrix equation construct where the **b** vector contained elements of the **x** vector. This required us to consider options like an iterative technique to solve for the **x** vector. We now examine an alternative the overcomes this characteristic.

Consider Eq. (50) which we now repeat here as

$$\mathbf{r}_{c,i}{}^{T}\mathbf{s} - \left|\mathbf{r}_{s,meas,i}\right| r_{bias} = \frac{1}{2}\left(\left|\mathbf{r}_{c,i}\right|^2 - \left(\left|\mathbf{r}_{s,meas,i}\right|\right)^2 + \left|\mathbf{s}\right|^2 - r_{bias}^2 \right), \tag{106}$$

Having also assumed a constant range bias, or

$$r_{bias,i} = r_{bias} \text{ = constant, albeit unknown.} \tag{107}$$

Let us now consider two such measurements from two independent SAR images, that is

$$\begin{aligned} &\mathbf{r}_{c,1}{}^{T}\mathbf{s} - \left|\mathbf{r}_{s,meas,1}\right| r_{bias} = \frac{1}{2}\left(\left|\mathbf{r}_{c,1}\right|^2 - \left(\left|\mathbf{r}_{s,meas,1}\right|\right)^2 + \left|\mathbf{s}\right|^2 - r_{bias}^2 \right), \text{ and} \\ &\mathbf{r}_{c,2}{}^{T}\mathbf{s} - \left|\mathbf{r}_{s,meas,2}\right| r_{bias} = \frac{1}{2}\left(\left|\mathbf{r}_{c,2}\right|^2 - \left(\left|\mathbf{r}_{s,meas,2}\right|\right)^2 + \left|\mathbf{s}\right|^2 - r_{bias}^2 \right). \end{aligned} \tag{108}$$

Taking the difference between these two equations yields the vector equation

$$\left[\left(\mathbf{r}_{c,2}{}^{T} - \mathbf{r}_{c,1}{}^{T}\right) \quad -\left(\left|\mathbf{r}_{s,meas,2}\right| - \left|\mathbf{r}_{s,meas,1}\right|\right) \right] \begin{bmatrix} \mathbf{s} \\ r_{bias} \end{bmatrix} = \frac{1}{2} \begin{pmatrix} \left|\mathbf{r}_{c,2}\right|^2 - \left|\mathbf{r}_{c,1}\right|^2 \\ -\left(\left|\mathbf{r}_{s,meas,2}\right|\right)^2 + \left(\left|\mathbf{r}_{s,meas,1}\right|\right)^2 \end{pmatrix}. \tag{109}$$

Note that the right-hand side of this equation no longer contains location vector **s**, or the range bias r_{bias}.

We now assemble several such pairs into a matrix equation

$$\mathbf{Ax} = \mathbf{b}, \tag{110}$$

where again

$$\mathbf{x} = \begin{bmatrix} \mathbf{s} \\ r_{bias} \end{bmatrix} = 4\times 1 \text{ column vector,} \tag{111}$$

but now

$$\mathbf{A} = \begin{bmatrix} \left(\mathbf{r}_{c,2}{}^T - \mathbf{r}_{c,1}{}^T\right) & -\left(\left|\mathbf{r}_{s,meas,2}\right| - \left|\mathbf{r}_{s,meas,1}\right|\right) \\ \left(\mathbf{r}_{c,4}{}^T - \mathbf{r}_{c,3}{}^T\right) & -\left(\left|\mathbf{r}_{s,meas,4}\right| - \left|\mathbf{r}_{s,meas,3}\right|\right) \\ \vdots & \vdots \\ \left(\mathbf{r}_{c,M}{}^T - \mathbf{r}_{c,M-1}{}^T\right) & -\left(\left|\mathbf{r}_{s,meas,M}\right| - \left|\mathbf{r}_{s,meas,M-1}\right|\right) \end{bmatrix} = \frac{M}{2} \times 4 \text{ matrix, and}$$

$$\mathbf{b} = \begin{bmatrix} \frac{1}{2}\left|\mathbf{r}_{c,2}\right|^2 - \left|\mathbf{r}_{c,1}\right|^2 - \left(\left|\mathbf{r}_{s,meas,2}\right|\right)^2 + \left(\left|\mathbf{r}_{s,meas,1}\right|\right)^2 \\ \frac{1}{2}\left|\mathbf{r}_{c,4}\right|^2 - \left|\mathbf{r}_{c,3}\right|^2 - \left(\left|\mathbf{r}_{s,meas,4}\right|\right)^2 + \left(\left|\mathbf{r}_{s,meas,3}\right|\right)^2 \\ \vdots \\ \frac{1}{2}\left|\mathbf{r}_{c,M}\right|^2 - \left|\mathbf{r}_{c,M-1}\right|^2 - \left(\left|\mathbf{r}_{s,meas,M}\right|\right)^2 + \left(\left|\mathbf{r}_{s,meas,M-1}\right|\right)^2 \end{bmatrix} = \frac{M}{2} \times 1 \text{ column vector.} \tag{112}$$

If data is collected so that **A** has full rank, we may calculate a least-squares solution as

$$\hat{\mathbf{x}} = \left(\mathbf{A}^T\mathbf{A}\right)^{-1}\mathbf{A}^T\mathbf{b}\,. \tag{113}$$

The $\hat{\mathbf{x}}$ vector then contains estimates of its constituents

$$\hat{\mathbf{x}} = \begin{bmatrix} \hat{\mathbf{s}} \\ \hat{r}_{bias} \end{bmatrix}. \tag{114}$$

We have constructed this the **A** matrix and **b** vector combination so that each row contains data from a unique pair of SAR images. That is, no rows share any data. To solve for four unknowns, this requires

$$M \geq 8\,, \text{ and } M \text{ even.} \tag{115}$$

The attractiveness of this is that there is no correlation between measurements in any of the elements of the **b** vector. This simplifies DOP calculations.

There is no overt reason for constructing the **A** matrix and **b** vector using adjacent images in each row. Any particular pairings would seem to provide the same result.

In fact, we might also have constructed the **A** matrix and **b** vector to use a common reference for subtraction, as

$$\mathbf{A} = \begin{bmatrix} \left(\mathbf{r}_{c,2}{}^T - \mathbf{r}_{c,1}{}^T\right) & -\left(\left|\mathbf{r}_{s,meas,2}\right| - \left|\mathbf{r}_{s,meas,1}\right|\right) \\ \left(\mathbf{r}_{c,3}{}^T - \mathbf{r}_{c,1}{}^T\right) & -\left(\left|\mathbf{r}_{s,meas,3}\right| - \left|\mathbf{r}_{s,meas,1}\right|\right) \\ \vdots & \vdots \\ \left(\mathbf{r}_{c,M}{}^T - \mathbf{r}_{c,1}{}^T\right) & -\left(\left|\mathbf{r}_{s,meas,M}\right| - \left|\mathbf{r}_{s,meas,1}\right|\right) \end{bmatrix} = (M-1)\times 4 \text{ matrix, and}$$

$$\mathbf{b} = \begin{bmatrix} \frac{1}{2}\left|\mathbf{r}_{c,2}\right|^2 - \left|\mathbf{r}_{c,1}\right|^2 - \left(\left|\mathbf{r}_{s,meas,2}\right|\right)^2 + \left(\left|\mathbf{r}_{s,meas,1}\right|\right)^2 \\ \frac{1}{2}\left|\mathbf{r}_{c,3}\right|^2 - \left|\mathbf{r}_{c,1}\right|^2 - \left(\left|\mathbf{r}_{s,meas,3}\right|\right)^2 + \left(\left|\mathbf{r}_{s,meas,1}\right|\right)^2 \\ \vdots \\ \frac{1}{2}\left|\mathbf{r}_{c,M}\right|^2 - \left|\mathbf{r}_{c,1}\right|^2 - \left(\left|\mathbf{r}_{s,meas,M}\right|\right)^2 + \left(\left|\mathbf{r}_{s,meas,1}\right|\right)^2 \end{bmatrix} = (M-1)\times 1 \text{ column vector.} \tag{116}$$

To solve for four unknowns, this then requires fewer SAR images; in fact only

$$M \geq 5. \tag{117}$$

The unattractiveness of this is that there is now correlation between measurements of the various elements of the **b** vector. This complicates DOP calculations somewhat, but does not prohibit it.

A similar technique is presented by Manolakis.[9]

"For a successful technology, reality must take precedence over public relations, for Nature cannot be fooled."
-- Richard P. Feynman

7 Factors Influencing Accurate Radar Ranging

A fundamental tenet of the subject of this report is that we can accurately 'measure' the range between the radar and a scatterer of interest; that we wish to geolocate. This measure is actually a calculation originating in an echo time-delay measurement, more actually a count of clock cycles of an underlying time base.

There are a number of mechanisms that can affect the accuracy and precision of a radar's ranging ability. Several are discussed in an earlier report.[5] We repeat and expand somewhat on the previous discussion here. Note that we limit our discussion to a monostatic radar architecture.

Motion measurement of the antenna phase center

When we consider a "range" from the radar to a scatterer location, at some point we need to decide "range from what?" That is, "Just how do we define the position of the radar?"

The natural point to define the radar location is the Antenna Phase Center (APC). This point location is mechanically related to the antenna structure, but not always obvious.[10] Nevertheless, it is fundamental to the geometry of radar ranging. It is the location of the APC that figures into any ranging measurements.

Any motion measurement of the radar, due to its navigation subsystem, needs to be translated to the APC by appropriate lever-arm calculations. This includes any GPS measurements, and any measurements by the Inertial Navigation System (INS). We opine that any lever-arms should be measurable to within a few cm.

Of course, even with perfect lever-arms, the accuracy and precision of the APC is limited by the accuracy and precision of the GPS-aided INS.[5] Anecdotal measurements suggest that a navigation subsystem should be able to achieve an overall RMS error of about 1 m. Over a short term a navigator error will look more like a position bias, becoming less correlated over time. Note that a position bias is not exactly the same as a range bias, especially when the angular perspective changes substantially.

Range/delay calibration to the antenna phase center

The gross delay that a radar measures includes not only the 2-way propagation delay between the radar APC and the scatterer location of interest, but also includes other system delays in the components of the electronic circuitry of the radar hardware. If left uncompensated, or otherwise unaccounted for, then this extra delay will manifest as a range bias or error, because it adds to the echo delay time between APC and scatterer.

This extra delay is typically measured via a calibration operation, and then subtracted from or otherwise compensated to the gross delay, so that the final "adjusted" delay is strictly between APC and scatterer.

It is critical that the range/delay calibration include the total signal propagation path (both transmit and receive) up to the APC, and not fall short to some other more convenient point in the signal path, such as to the antenna port, or feed structure, etc. It needs to be to the APC. It

also needs to include any latencies in command timing and control. We opine that any range/delay calibration can probably be made to equivalently within a few cm.

Target correspondence in the images

When multilateration is used involving multiple SAR images, the tacit assumption is that the same scatterer location can be accurately identified in all the images. This is the "correspondence" issue. Even a readily identifiable isotropic point scatterer may straddle pixels differently in different images.

We opine that using a simple "maximum pixel" selection for a point scatterer, or equivalent such as a trihedral corner reflector, can locate such a scatterer to within half a pixel spacing. The standard deviation for any error will then be about 30% of the pixel spacing, based on a uniform distribution. For a pixel spacing of 10 cm, this amounts to a standard deviation of about 3 cm.

Atmospheric propagation effects

Propagation of a radar signal through the Earth's atmosphere will be somewhat slower than in free space, and will depend on specific atmospheric conditions. This is discussed in some detail in an earlier report,[3] and is summarized in Appendix C.

We observe that for a typical atmosphere, and a radar height above the ground of about 3000 m, the range bias will be about 260 ppm, with a standard deviation of about 22 ppm. Note that this standard deviation is in regard to the bias, and is expected to exhibit a high degree of correlation between SAR images collected from the same overall flightpath. Note further that this scales with range. For example, at a 20 km slant range, this amounts to a 5.2 m bias with respect to free space, with a standard deviation of about 44 cm.

Other errors

A number of other factors can also influence the accuracy and precision of a range measurement. These might include

- SAR image focus issues can impact pixel selection accuracy for scatterer feature location.
- Clock errors, in the basic system time base, can affect the accuracy of the measure of time. We note that clock stability will depend on temperature and aging, among other things. Stability in a high-quality oscillator might typically be limited to 10 ppm.
- SAR image geometric distortions may impact ranging calculations.
- Glint and scintillation may impact pixel selection from one SAR image to the next.
- SAR, like most radar systems, employs the Born approximation,[12] where echoes are generally assumed to be direct. Multipath effects can influence pixel selection accuracy.

There are probably other sources of errors, too.

Combined Ranging Errors

The errors discussed above are generally independent of each other. Therefore, we may examine their combined effects statistically by a Root Sum Squared (RSS) analysis.

Except for navigation errors and atmospheric propagation velocity errors, everything else tends to exhibit standard deviations in the few centimeter range. Consequently, with the typical standard deviations previously discussed, even at 20 km range we might expect a net combined standard deviation of perhaps 1.1 m or so around the nominal atmospheric propagation bias level. Even much of this error will manifest as principally a residual range bias, rather than uncorrelated "measurement noise." Of course, these are statistical numbers. Assuming a net Gaussian distribution, then about 68% of the time we should be below this. Figure 8 shows how the standard deviation in range error might vary with range. Actual range "noise" for temporally close SAR images is probably in the several centimeter range.

So, if our range/delay calibration is off by 20 cm or so (maybe calibrating just to the feed and not the APC), and radar navigation is off by 10-20 cm by measuring to something other than the APC, then these errors become very significant very quickly.

We emphasize that geolocation accuracy without truth data can at best be described statistically. Confidence in the statistics, however, requires a statistically significant number of experiments, where ranging is in fact evaluated against truth data.

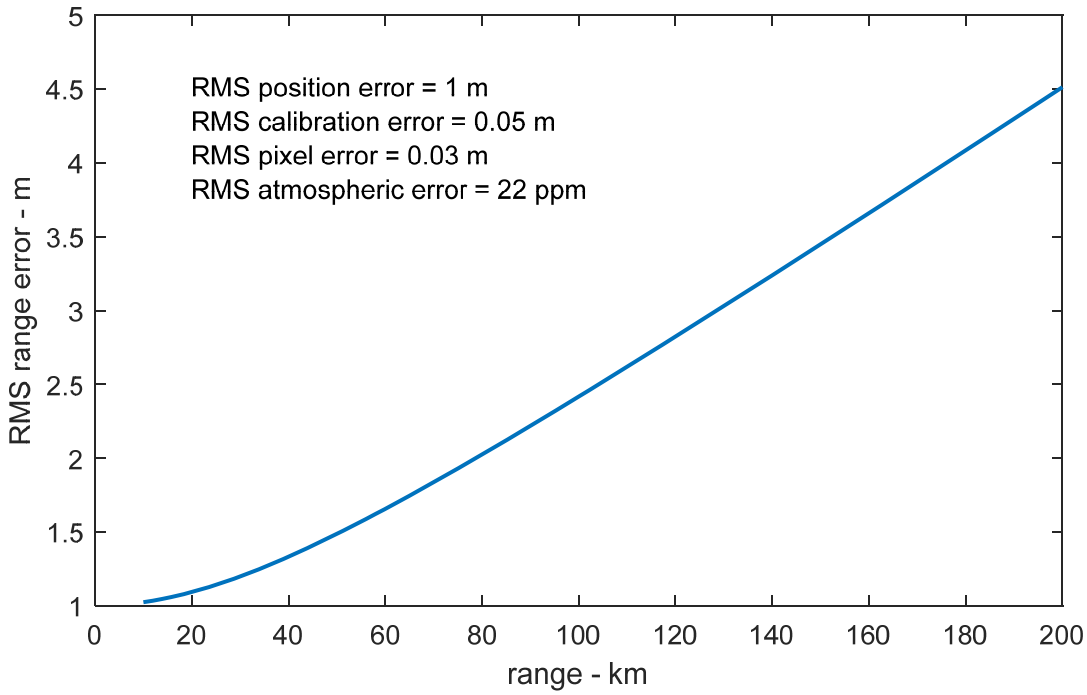

Figure 8. RMS range error as a function of range. Radar is assumed at 3000 m altitude.

“There is a great satisfaction in building good tools for other people to use.”
-- Freeman Dyson

8 Conclusions

We offer and repeat some key points.

- Radar is first and foremost a ranging operation.
- Range measurements from multiple aspects can be combined to calculate a 3-D location for a scatterer. This is called multilateration.
- If multiple range measurements over-constrain the solution, then a least-squares solution can be calculated. If measurement error statistics vary widely, then a weighted least-squares solution might be calculated.
- Some data collections geometries are not suitable for multilateration, like colinear or coplanar ranging measurements.
- Range biases due to atmospheric propagation characteristics are particularly problematic. Everything works best if resulting range biases can be largely compensated before any geolocation calculations.
- Range biases might also be estimated from the data, but doing so adds yet additional constraints on data collection geometries. For example, constant range orbiting flightpaths become problematic.
- Extra constraints can be built into the calculations to effectively "tether" some parameters so that solutions don't blow up.
- A useful measure for the goodness of a collection geometry is "Dilution of Precision."

We additionally observe that more independent information can significantly aid the precision and accuracy with which we might geolocate a scatterer. An obvious candidate for this is the range-rate information within a synthetic aperture for each SAR image, manifesting as the azimuth offset of a scatterer from the SRP. This will be the topic of a subsequent report.[13]

Figure 9. Campsite in the mountains (courtesy Miss Taylor Spaulding, 7 ½).

Appendix A – Basic Linear Algebra

We present here some basic linear algebra concepts. Ample texts and publications exist that cover these concepts in detail.[14,15,16,17]

We begin with the conventional linear system of equations given in matrix form as

$$\mathbf{A}\mathbf{x} = \mathbf{b}\,, \tag{A1}$$

where

$\mathbf{A}$ = $M \times N$ matrix,
$\mathbf{x}$ = $N \times 1$ column vector, and
$\mathbf{b}$ = $M \times 1$ column vector. (A2)

Matrix $\mathbf{A}$ and vector $\mathbf{b}$ are known. We wish to solve for unknown vector $\mathbf{x}$.

If $\mathbf{A}$ is square and full rank, we can solve

$$\mathbf{x} = \mathbf{A}^{-1}\mathbf{b}\,. \tag{A3}$$

If the system is over-constrained, but still has full rank, we can solve

$$\mathbf{x} = \left(\mathbf{A}^T\mathbf{A}\right)^{-1}\mathbf{A}^T\mathbf{b}\,. \tag{A4}$$

We note that Eq. (A4) reduces to Eq. (A3) for a square matrix $\mathbf{A}$. The entity $\left(\mathbf{A}^T\mathbf{A}\right)^{-1}\mathbf{A}^T$ is sometimes called the pseudo-inverse of $\mathbf{A}$, or the Moore–Penrose pseudoinverse matrix of $\mathbf{A}$.

Some additional useful matrix identities include for generic matrices $\mathbf{G}$ and $\mathbf{H}$,

$$\begin{aligned}
&\left(\mathbf{GH}\right)^T = \mathbf{H}^T\mathbf{G}^T\,,\\
&\left(\mathbf{GH}\right)^{-1} = \mathbf{H}^{-1}\mathbf{G}^{-1}, \quad \text{if individual inverses exist,}\\
&\left(\mathbf{G}^T\right)^{-1} = \left(\mathbf{G}^{-1}\right)^T\,.
\end{aligned} \tag{A5}$$

A weighted least squares solution to Eq. (A1) may be found by solving

$$\mathbf{W}\,\mathbf{A}\,\mathbf{x} = \mathbf{W}\,\mathbf{b}\,, \tag{A6}$$

where the weight matrix is

$$\mathbf{W} \text{ = diagonal matrix of weights for uncorrelated errors in } \mathbf{b}. \tag{A7}$$

Note that because it is diagonal, $\mathbf{W}$ is the same as its transpose, that is

$$\mathbf{W}^T = \mathbf{W}. \tag{A8}$$

The solution to Eq. (A6) becomes

$$\mathbf{x} = \left(\mathbf{A}^T \mathbf{W}\, \mathbf{A} \right)^{-1} \mathbf{A}^T \mathbf{W}\, \mathbf{b}\,, \tag{A9}$$

This is then the weighted least squares solution to Eq. (A1).

Weighting is used to essentially favor more accurate observations at the expense of less accurate observations. Weights are often proportional to the inverse of the variance of respective observations.

Appendix B – Dilution of Precision (DOP)

The concept of Dilution of Precision (DOP) is essentially a figure of merit that is an error sensitivity estimation or calculation. It is common for the Global Positioning System (GPS).[18]

We continue with the definitions of Appendix A. We recall the conventional linear system of equations given in matrix form as

$$\mathbf{A}\mathbf{x} = \mathbf{b}\,. \tag{B1}$$

Recall that if **A** is full rank, we can solve

$$\mathbf{x} = \left(\mathbf{A}^T\mathbf{A}\right)^{-1}\mathbf{A}^T\mathbf{b}\,, \tag{B2}$$

which works even whether or not **A** is square. For convenience we will rewrite Eq. (B2) as

$$\mathbf{x} = \mathbf{C}\,\mathbf{b}\,, \tag{B3}$$

where

$$\mathbf{C} = \left(\left(\mathbf{A}^T\mathbf{A}\right)^{-1}\mathbf{A}^T\right). \tag{B4}$$

We note that for a weighted least squares solution

$$\mathbf{C} = \left(\left(\mathbf{A}^T\mathbf{W}\,\mathbf{A}\right)^{-1}\mathbf{A}^T\mathbf{W}\right). \tag{B5}$$

Now, an error in vector **b** will yield an error in the solution to vector **x**. That is

$$\left(\mathbf{x} + \boldsymbol{\varepsilon}_x\right) = \mathbf{C}\left(\mathbf{b} + \boldsymbol{\varepsilon}_b\right), \tag{B6}$$

where the individual error vectors are defined as

$$\begin{aligned} \boldsymbol{\varepsilon}_b &= \text{column vector of errors in } \mathbf{b}, \text{ and} \\ \boldsymbol{\varepsilon}_x &= \text{column vector of errors in } \mathbf{x}, \end{aligned} \tag{B7}$$

which of course means that the errors are related as

$$\boldsymbol{\varepsilon}_x = \mathbf{C}\boldsymbol{\varepsilon}_b\,. \tag{B8}$$

Covariances can be calculated as

$$E\left\{\boldsymbol{\varepsilon}_x \boldsymbol{\varepsilon}_x{}^T\right\} = \mathbf{C} E\left\{\boldsymbol{\varepsilon}_b \boldsymbol{\varepsilon}_b{}^T\right\} \mathbf{C}^T , \tag{B9}$$

where the expected value function is defined as

$$E\{z\} \text{ = expected value of } z. \tag{B10}$$

We may write Eq. (B9) somewhat more succinctly as

$$\boldsymbol{\Sigma}_x = \mathbf{C}\, \boldsymbol{\Sigma}_b\, \mathbf{C}^T , \tag{B11}$$

where

$$\begin{aligned} \boldsymbol{\Sigma}_x &= E\left\{\boldsymbol{\varepsilon}_x \boldsymbol{\varepsilon}_x{}^T\right\} \text{ = covariance matrix for } \boldsymbol{\varepsilon}_x \text{, and} \\ \boldsymbol{\Sigma}_b &= E\left\{\boldsymbol{\varepsilon}_b \boldsymbol{\varepsilon}_b{}^T\right\} \text{ = covariance matrix for } \boldsymbol{\varepsilon}_b . \end{aligned} \tag{B12}$$

Now for some special cases.

Case 1.

In this case, we stipulate equal independent variances in the **b** vector, so that

$$\boldsymbol{\Sigma}_b = \sigma_{ref}^2 \mathbf{I} , \tag{B13}$$

where

$$\sigma_{ref}^2 \text{ = variance of the individual entries in } \mathbf{b}\text{, common to all elements.} \tag{B14}$$

In this case, and assuming an unweighted solution where $\mathbf{W} = \mathbf{I}$,

$$\boldsymbol{\Sigma}_x = \sigma_{ref}^2 \left(\mathbf{C}\, \mathbf{C}^T\right) = \sigma_{ref}^2 \left(\mathbf{A}^T \mathbf{A}\right)^{-1} . \tag{B15}$$

Normalizing to σ^2 yields

$$\frac{\boldsymbol{\Sigma}_x}{\sigma_{ref}^2} = \left(\mathbf{A}^T \mathbf{A}\right)^{-1} . \tag{B16}$$

The diagonal elements of $\boldsymbol{\Sigma}_x \big/ \sigma_{ref}^2$ are ratios of variances. The square-root of these ratios are relative standard deviations. So, the square-root of the diagonal elements of

$\boldsymbol{\Sigma}_x \big/ \sigma_{ref}^2$ represent a scaling of standard deviations, that is, a scaling of precision due to errors in **b**. These are the DOP values.

Case 2.

In this case, we stipulate independent unequal variances in the **b** vector, so that

$$\boldsymbol{\Sigma}_b = \sigma_{ref}^2 \mathbf{K}\,, \tag{B17}$$

where

σ_{ref}^2 = reference variance of the individual entries in **b**, and

K = diagonal matrix of weights meant to scale σ_{ref}^2. (B18)

Since σ_{ref}^2 is a somewhat arbitrary reference value, elements of **K** may generally be more or less than one. In this case, the covariance matrix for $\boldsymbol{\varepsilon}_x$ becomes

$$\boldsymbol{\Sigma}_x = \sigma_{ref}^2 \left(\mathbf{C}\, \mathbf{K} \mathbf{C}^T \right). \tag{B19}$$

Normalizing to σ_{ref}^2 yields

$$\frac{\boldsymbol{\Sigma}_x}{\sigma_{ref}^2} = \mathbf{C}\, \mathbf{K} \mathbf{C}^T. \tag{B20}$$

When the variances in $\boldsymbol{\Sigma}_b$ are not equal,[‡‡] then it is common to use a weighted least squares solution where the weights are the reciprocal of the variance of the observations. This essentially favors more accurate observations at the expense of less accurate observations, providing overall minimum variances in the output covariance matrix $\boldsymbol{\Sigma}_x$. This means

$$\mathbf{W} = \mathbf{K}^{-1}, \tag{B21}$$

in which case Eq. (B20) reduces to

$$\frac{\boldsymbol{\Sigma}_x}{\sigma_{ref}^2} = \left(\mathbf{A}^T \mathbf{W}\, \mathbf{A} \right)^{-1}. \tag{B22}$$

[‡‡] A diagonal $\boldsymbol{\Sigma}_b$ with unequal elements is termed heteroscedasticity.

The diagonal elements of $\boldsymbol{\Sigma}_x \big/ \sigma_{ref}^2$ are still ratios of variances. So, the square-root of the diagonal elements of $\boldsymbol{\Sigma}_x \big/ \sigma_{ref}^2$ are still the DOP values, with the constraint that they are relative to a reference error in **b**.

Some DOP values, or combinations of DOP values, have been given specific nomenclature.

If elements of vector **x** represent position, with *x* and *y* coordinates representing horizontal positions, and *z* representing a vertical position coordinate, and the diagonal elements of $\boldsymbol{\Sigma}_x$ are

$$\text{diag}\left(\boldsymbol{\Sigma}_x\right) = \begin{bmatrix} \sigma_x^2 & \sigma_y^2 & \sigma_z^2 \end{bmatrix}^T, \tag{B23}$$

then

$$\begin{aligned} &\text{HDOP = Horizontal DOP} = \sqrt{\left(\sigma_x^2 + \sigma_y^2\right) \big/ \sigma_{ref}^2}\ , \\ &\text{VDOP = Vertical DOP} = \sqrt{\sigma_z^2 \big/ \sigma_{ref}^2}\ , \\ &\text{PDOP = Position DOP} = \sqrt{\left(\sigma_x^2 + \sigma_y^2 + \sigma_z^2\right) \big/ \sigma_{ref}^2} \end{aligned} \tag{B24}$$

Other DOP values are also employed. For example, GPS figure of merits also include Time DOP (TDOP) and Geometric DOP (GDOP).

Appendix C – Range Bias Due to Atmosphere

A principal source for a radar ranging error is the range bias introduced by propagation of the radar signal in the atmosphere. This is discussed in some detail in an earlier report.[3] The propagation velocity of the radar waveform depends on the refractivity of the atmosphere, which depends on atmospheric constituents and conditions (mainly humidity), and generally decreases exponentially with altitude.

In this appendix, we summarize some key points from the aforementioned report, and illustrate a reasonable model for estimating range bias due to atmospheric propagation.[§§]

From the earlier report, we will assume an exponential decay of refractivity with altitude, namely

$$N(h) = N_s \, e^{\frac{-(h-h_s)}{H_b}}, \tag{C1}$$

where

N_s = reference surface refractivity in N-units,
h = altitude of interest,
h_s = altitude of reference surface., and
H_b = decay factor. (C2)

The actual proper index of refraction is calculated as

$$n(h) = 1 + 10^{-6} N(h). \tag{C3}$$

The decay factor is itself a function,

$$H_b = \frac{h_b - h_s}{\ln\left(\frac{N_s}{N_b}\right)}. \tag{C4}$$

We will presume that our interest is principally over an altitude range of 0 to 50 kft (15240 m), so we might choose fit coefficients to be

$h_b = 40\,\text{kft} = 12192\,\text{m}$, and
$N_b = 66.65$ N-units. (C5)

[§§] We're talking the Earth's atmosphere here.

We shall presume that an average propagation velocity between airborne radar and ground surface is reasonably inversely proportional to an average index of refraction, namely

$$c_{avg} = c_0 \left[1 + \frac{H_b 10^{-6} N_s}{(h_a - h_s)} \left(1 - e^{\frac{-(h_a - h_s)}{H_b}} \right) \right]^{-1}, \tag{C6}$$

where

$$c_0 = 299792458 \text{ m/s} = \text{free-space velocity of propagation.} \tag{C7}$$

This means that a radar range that is calculated using free-space velocity of propagation, will exhibit a range bias

$$r_{bias} \approx \frac{H_b 10^{-6} N_s}{(h_a - h_s)} \left(1 - e^{\frac{-(h_a - h_s)}{H_b}} \right) r_{s,meas}, \tag{C8}$$

where

$$r_{s,meas} = \text{the range calculated using free-space velocity.} \tag{C9}$$

This bias is positive, yielding a true range that is shorter than the "measured" range $r_{s,meas}$.

In anticipation of subsequent plots, we define a normalized range bias factor as

$$\beta = \frac{r_{bias}}{r_{s,meas}} \approx \frac{H_b 10^{-6} N_s}{(h_a - h_s)} \left(1 - e^{\frac{-(h_a - h_s)}{H_b}} \right) = \text{range bias factor.} \tag{C10}$$

Variation in Surface Refractivity

The surface refractivity N_s will depend on atmospheric constituents and conditions, including temperature, pressure, and humidity.

An average value for N_s for the continental US is given by Bean[19] as 313 N-units, whereas Altshuler[20] reports that his data shows that "the average global surface refractivity is 324.8 N-units and that the standard deviation of [his] sample is 30.1 N-units." A report by Robertshaw[21] in support of the Joint STARS program shows mean values for surface refractivity are in the range of 330 with a standard deviation in the range of 20 or so.

We might expect values for N_S to range from 250 N-units at higher altitudes and cooler temperatures, to perhaps 400 N-units at sea level on a warm day.

Variation in Range Bias

The variations in surface refractivity may be combined with Eq. (C10) to allow us to examine expected variations in range bias factor, and ultimately range bias itself.

Figure 10 shows how the range bias factor changes with radar altitude, for a span of surface refractivity N_S. Note how the range bias factors decrease with radar altitude.

Figure 11 shows how a standard deviation in range bias factor also decreases with altitude.

Example

> From these plots, we may estimate for an altitude of 10 kft (3048 m), for a typical atmosphere with 313 N-units of surface refractivity, the range bias factor is about 260 ppm, with a standard deviation of about 22 N-units. At a slant-range of 20 km, this translates to a range bias of about 5.2 m, with a standard deviation of about 0.44 m.

Comments

We offer several comments on this model.

- The coefficients chosen in Eq. (C5) fit well to the altitude range of 0 to 50 kft (15240 m). We allow that they may be optimized to different values for other altitude ranges.
- We also allow that other, perhaps no less accurate models, may exist that might amply serve the purpose herein.
- The model summarized here (developed in an earlier report[3]) is based on a rather simple, though often reasonably adequate, model for refractivity with altitude, given in Eq. (C1). In this sense, the atmosphere is rarely if ever what we might refer to as "typical." We acknowledge that this model ignores many complexities of the atmosphere that might affect propagation, such as ducting or boundary layer effects.[22]
- We opine that SAR images should record in their metadata any atmospheric propagation corrections made in their formation, sufficient for their removal or modification if better atmospheric propagation information becomes available.

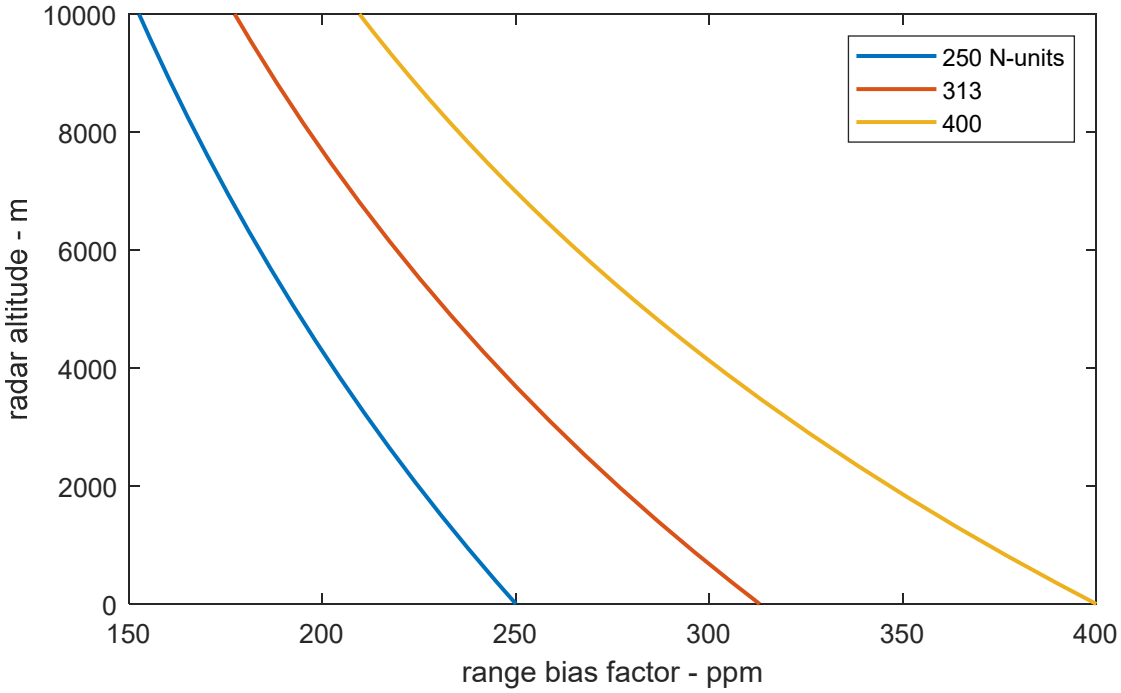

Figure 10. Relationship of range bias factor with altitude for various surface refractivities.

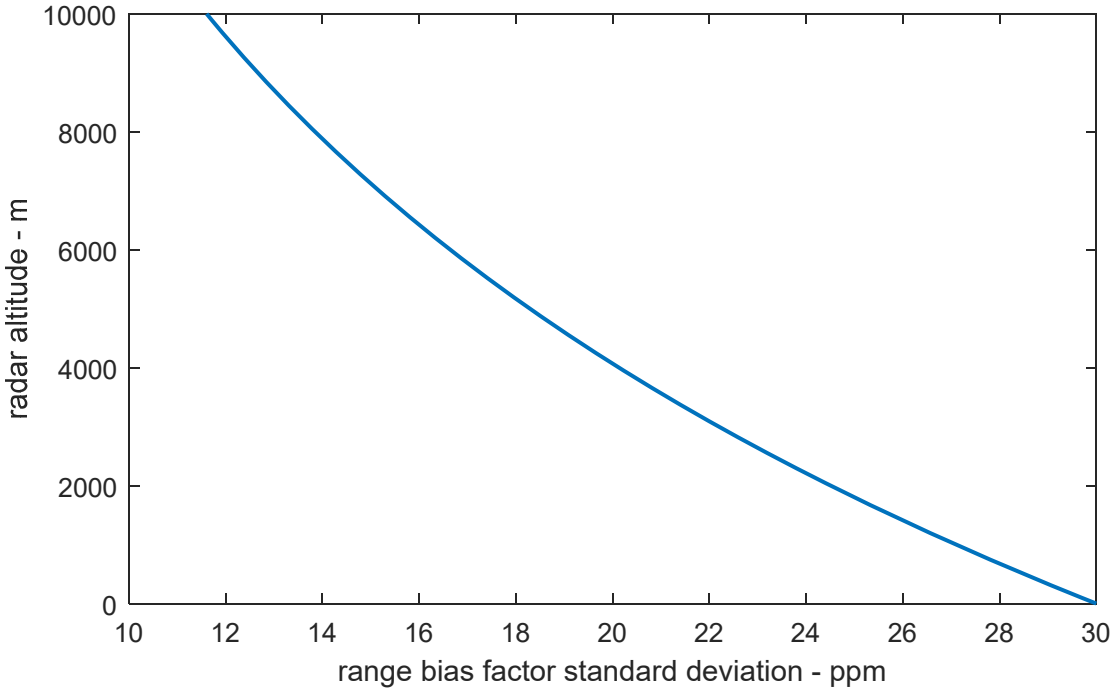

Figure 11. Estimated standard deviation of range bias factor as a function of altitude.

Reference

[1] Armin W. Doerry, *3-D Target Location from Stereoscopic SAR Images*, Sandia National Laboratories Report SAND99-2643, October 1999.

[2] John M. DeLaurentis, Armin W. Doerry, *Stereoscopic Height Estimation from Multiple Aspect Synthetic Aperture Radar Images*, Sandia National Laboratories Report SAND2001-2585, August 2001.

[3] Armin W. Doerry, *Radar Range Measurements in the Atmosphere*, Sandia National Laboratories Report SAND2013-1096, Unlimited Release, February 2013.

[4] Armin W. Doerry, *Earth Curvature and Atmospheric Refraction Effects on Radar Signal Propagation*, Sandia National Laboratories Report SAND2012-10690, Unlimited Release, January 2013.

[5] Armin W Doerry, Douglas L Bickel, *Radar Motion Measurements and Synthetic Aperture Radar Image Geolocation Accuracy*, Sandia National Laboratories Report SAND2020-10779, Unlimited Release, October 2020.

[6] Armin W Doerry, Douglas L Bickel, *Synthetic Aperture Radar Height of Focus*, Sandia National Laboratories Report SAND2021-0144, Unlimited Release, January 2021.

[7] William Mark Wonnacott, *Geolocation with Error Analysis Using Imagery from an Experimental Spotlight SAR*, Purdue University, West Lafayette, Indiana, December 2008.

[8] *Spotlight Synthetic Aperture Radar (SAR) Sensor Model Supporting Precise Geopositioning*, Version 1.0, NGA Standardization Document, NGA.SIG.0005_1.0, 30 March 2010.

[9] D. E. Manolakis, "Efficient solution and performance analysis of 3-D position estimation by trilateration," *IEEE Transactions on Aerospace and Electronic Systems*, Vol. 32, No. 4, October, 1996.

[10] Armin W. Doerry, *Just Where Exactly is the Radar? (a.k.a. The Radar Antenna Phase Center)*, Sandia National Laboratories Report SAND2013-10635, Unlimited Release, December 2013.

[11] H. L. Van Trees, *Optimum Array Processing: Part IV of Detection, Estimation, and Modulation Theory*, ISBN-13: 978-0471093909, John Wiley & Sons, Inc., 2002.

[12] Joseph W. Goodman, *Statistical Optics*, ISBN 0-471-01502-4, John Wiley & Sons, Inc., 1985.

[13] Armin W Doerry, Douglas L Bickel, *SAR Geolocation Using Range-Doppler Multilateration*, Sandia National Laboratories Report, to be published.

[14] Gilbert Strang, *Linear Algebra and its Applications*, ISBN 0-12-673660-X, Academic Press, Inc., 1976, 1980.

[15] Philippe G. Ciarlet, *Introduction to Numerical Linear Algebra and Optimisation*, ISBN 0-521-33984-7, Cambridge University Press, 1989, 1991.

[16] Gene H. Golub, Charles F. Van Loan, *Matrix Computations*, second edition, ISBN 0-8018-3739-1, The Johns Hopkins University Press, 1989, 1991.

[17] Daniel T. Finkbeiner II, *Introduction to Matrices and Linear Transformations*, third edition, ISBN 0-7167-0084-0, W. H. Freeman and Company, 1960, 1966, 1978.

[18] Elliott D. Kaplan (editor), *Understanding GPS Principles and Applications*, ISBN 0-89006-793-7, Arthech House, Inc., 1996.

[19] Bradford R. Bean, "The Radio Refractive Index of Air", *Proceedings of the I.R.E.*, Vol. 50, Issue 3, pp. 260-273, March 1962.

[20] Edward E. Altshuler, "Tropospheric Range-Error Corrections for the Global Positioning System", *IEEE Transactions on Antennas and Propagation*, Vol. 46, No 5, pp. 643-649, May 1998.

[21] G. A. Robertshaw, "Range Corrections for Airborne Radar - A Joint STARS Study", Project No. 6460, Report number MTR-9055, ESD-TR-84-169, The MITRE Corporation, May 1984.

[22] Fred M. Dickey, Armin W. Doerry, Louis A. Romero, "Degrading effects of the lower atmosphere on long range airborne SAR imaging," *IET Proceedings on Radar, Sonar & Navigation*, Vol. 1, No. 5, pp. 329–339, October 2007.

“A child of five would understand this. Send someone to fetch a child of five.”
-- Groucho Marx

Distribution

Unlimited Release

Email—External

Brandeis Marquette	Brandeis.Marquette@ga-asi.com	General Atomics ASI
Jean Valentine	Jean.Valentine@ga-asi.com	General Atomics ASI
John Fanelle	John.Fanelle@ga-asi.com	General Atomics ASI

Email—Internal

all members	534x	
Technical Library	9536	libref@sandia.gov

Sandia National Laboratories is a multimission laboratory managed and operated by National Technology & Engineering Solutions of Sandia LLC, a wholly owned subsidiary of Honeywell International Inc. for the U.S. Department of Energy's National Nuclear Security Administration under contract DE-NA0003525.